Very High Density Sensing Arrays

Christopher N. LaFratta, and David R. Walt

Chem. Rev., **2008**, 108 (2), 614-637 • DOI: 10.1021/cr0681142

Very High Density Sensing Arrays

Christopher N. LaFratta and David R. Walt*

Department of Chemistry, Tufts University, 62 Talbot Avenue, Medford, Massachusetts 02155

Received April 3, 2007

Contents

1. Introduction

Historically, measurements have been made by taking a sample and analyzing it for a single analyte. When multiple analytes must be measured from a single sample, the sample conventionally is divided into appropriate aliquots and each aliquot is analyzed for a single analyte. This approach is exemplified by many of the clinical analyzers employed in today's modern hospital laboratories. Entire diagnostic panels are obtained from a single milliliter of blood by dividing the sample into dozens of channels that are analyzed for individual analytes such as Na^+, K^+, glucose, cholesterol, creatinine, uric acid, lactate dehydrogenase, and other clinically relevant analytes.

As more sophisticated scientific instrumentation developed, the ability to detect multiple substances simultaneously became routine. Multiple metals can be measured using atomic emission and absorption spectrometers. Hyphenated methods such as GC-MS enable the separation of a sample into its components followed by identification of each component. While these instruments have tremendous capabilities, they tend to be large, power-hungry, and require routine maintenance. Consequently, most of these instruments are relegated to a central laboratory staffed by scientists and technicians.

At the other extreme, simple colorimetric tests have been around for over a century. For example, litmus paper for determining acidity or basicity morphed into pH dipsticks in which different dyes were impregnated onto different pieces of filter paper, glued onto a plastic backing, and cut into strips containing multiple pH indicators. Similarly, dipsticks for measuring multiple analytes in swimming pools have been developed. These test strips were probably the first type of array, even though they were never recognized as such.

In the last several decades, sensors have become a staple of analytical research and been used increasingly for making quantitative measurements. Initially, single sensors were used to measure a single analyte. Eventually multiple sensors were bundled either to provide a multianalyte measurement capability or to obtain spatial measurements of a single analyte. During the same time frame, scientists began to work at the microscale and have since progressed to the nanoscale. Opportunities in nanoscience and nanotechnology, as well as improved microscale capabilities, are driving feature sizes down. As scientists have become more comfortable working at these scales, the thinking has shifted with the developing capability to put increasing functionality into smaller and smaller spaces. This capability is exemplified by the computer chip industry.

A direct outgrowth of small feature sizes has been the movement of the analytical community toward arrays. By developing methods to place different substances in different locations on a given substrate, it has become possible to produce arrays that contain many sensors or probes in a small area. These multifunctional devices enable multiple measure-

* To whom correspondence should be addressed. Phone: (617) 627-3470. Fax: (617) 627-3443. E-mail: david.walt@tufts.edu.

10.1021/cr0681142 CCC: $71.00
Published on Web 01/30/2008

Christopher LaFratta was born in Malden, MA, in 1979. He received his B.S. degree in Chemistry from the University of Massachusetts, Dartmouth in 2001. He then joined the laboratory of Professor John Fourkas at Boston College, where his research focused on various aspects of multiphoton fabrication. Having moved with Professor Fourkas to the University of Maryland, College Park, he received his Ph.D. degree in Chemistry from UMCP in 2006. He then joined the laboratory of Professor David Walt at Tufts University, where he was awarded a NIH/NIGMS postdoctoral fellowship. His current research involves the development of a microarray-based optoelectronic chemical sensing platform.

David R. Walt is Robinson Professor of Chemistry at Tufts University and a Howard Hughes Medical Institute Professor. He received his B.S. degree in Chemistry from the University of Michigan and Ph.D. degreevin Chemical Biology from SUNY at Stony Brook. After postdoctoral studies at MIT, he joined the chemistry faculty at Tufts. He served as Chemistry Department Chairman from 1989 to 1996. He serves on many government advisory panels and boards and on editorial advisory board for numerous journals. From 1996–2003 he was Executive Editor of *Applied Biochemistry and Biotechnology*. He is the Scientific Founder and Director of Illumina Inc. and Quanterix Corp. He has received numerous national and international awards and honors for his fundamental and applied work in the field of optical sensors and arrays and is a fellow of the American Association for the Advancement of Science. He has published over 200 papers, holds over 50 patents, and has given hundreds of invited scientific presentations.

ments to be made simultaneously by simply bringing a sample into contact with the array. As the feature sizes of arrays have decreased, the term "microarray" has become commonplace. Microarrays, with probes spotted onto a solid support, have revolutionized molecular biology and ushered in the '-omics' era. These arrays traditionally have densities of $\sim$50 spots/mm^2, with spots on the order of 100 μm in diameter, although some smaller spots have been reported.[1] A number of good reviews have been written about these 'high density' microarrays,[2−4] but here we will focus on newer array technologies enabling significantly higher densities.

This review deals with arrays containing the smallest feature sizes and the highest densities; hence, its title Very High Density Sensing Arrays. The motivation to create very high density sensing arrays is driven by several fronts. Increasing data are needed to solve increasingly complex problems. The field of Systems Biology has created a need to collect an enormous amount of data to understand the interactions and connections between biological pathways. The completions of the Human Genome Project and the HapMap Project have provided a rich database of human variation. Only by collecting millions of pieces of data from many thousands or millions of individuals will scientists be able to uncover the causes of disease and recommend changes in lifestyle to avoid them. Very high density sensing arrays enable the collection of large amounts of data. Fortunately, the tools exist for both collecting and processing large amounts of high-resolution data rapidly. For example, electronic components such as CCD chips, CMOS devices, and high-density integrated circuits provide the ability to collect enormous amounts of data on short time scales. Data storage capacity has increased to enable these data to be collected and stored. In addition, the ability to process data rapidly has kept pace. Without these corresponding improvements in data storage and processing capability, there would be no need to collect more data.

As discussed in this review, very high density arrays are beginning to change the way we make measurements, process the data from these measurements, and use the information that can be extracted from these data. Very high density sensing arrays will have applications in many fields including diagnostics, the environment, industrial processing, fundamental science, and many others.

1.1. Terminology

Martin and co-workers first used the term ensemble to describe the electrodes they fabricated by filling the pores of a membrane with metal. The term nanoelectrode ensemble (NEE) was used, rather than nanoelectrode array, because the pores of the template were not "evenly spaced".[5] Here we will use the term ensemble to mean a grouping of like sensor elements that respond collectively. The response of individual sensor elements in an ensemble, therefore, cannot be queried; instead, a collective signal is obtained from the entire ensemble. Unlike ensembles, the components of an array need not be identical and each can provide its own signal for detection.

Arrays can be made by many different techniques, but in all cases the resulting array will fall into one of two categories: directed arrays or randomly ordered arrays. An experiment that uses a 96-well plate is an example of a directed array because the materials inside each well are known and purposefully placed. This situation is not the case for a randomly ordered array, where the elements self-assemble into a pattern that is not preordained. A random array can be made by filling a template with different elements, such as filling microwells with beads having different surface chemistries. Here, the location of each bead in the array is random. It is then necessary to 'decode' the position and identity of each element to use it as a sensing array.

Another way to distinguish arrays from one another is based on the density of their elements. This article will focus on 'very high density' arrays, which qualitatively implies a density too high to manage without a computer. Quantita-

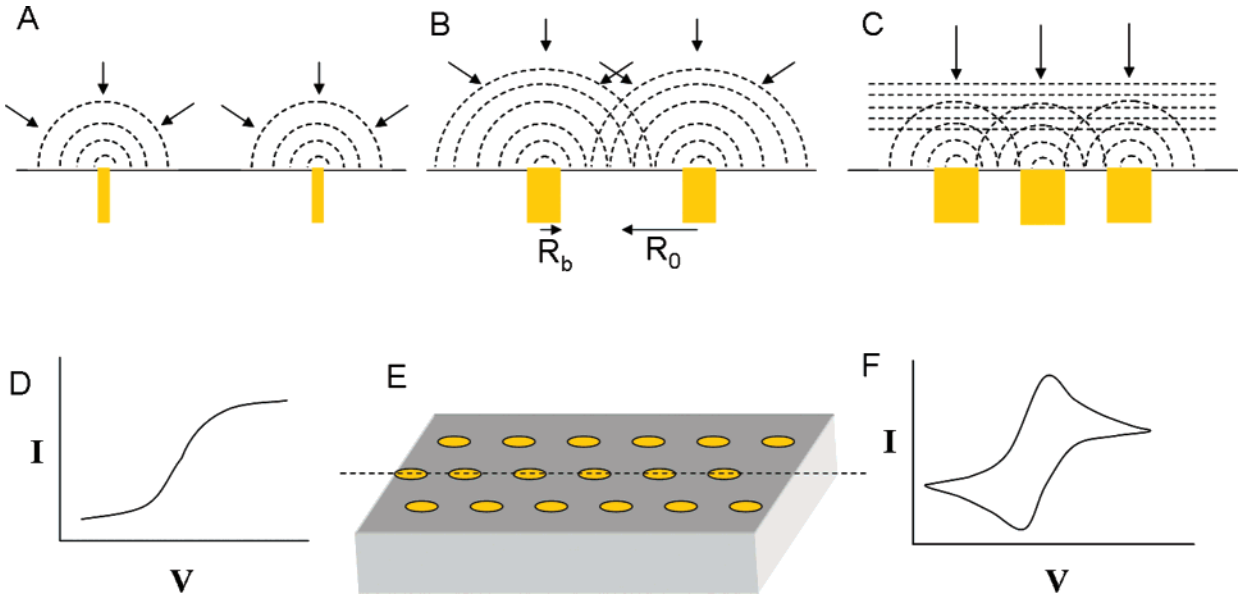

Figure 1. Schematic of electrode ensembles of different size and density showing (A) radial diffusion, (B) overlapping radial diffusion, and (C) planar diffusion. (D and F) Cyclic voltammograms for the diffusion scenario in A and C, respectively. (E) Electrode ensemble with metal electrodes represented by yellow circles surrounded by gray insulating material. Microelectrode radius, R_b, and diffusion zone radius, R_0, are shown.

tively, we define a very high density array to be one that contains more than 1000 elements per mm^2. This specification dictates that each feature on the array is spaced approximately 30 μm apart or less. Data obtained from even a modestly sized (1 cm^2) array would contain more than 100 000 array features. Such data sets, with hundreds of thousands to millions of data points, necessitate computer processing; drawing meaningful correlations among data of this size is beyond human capability.

This definition of very high density arrays based on element size invites a discussion of another class of array, known as suspension arrays, into this review. The elements of a suspension are not fixed in position but float freely in solution, and the size of the elements is generally about 5 μm or less. As in randomly ordered arrays, the elements of a suspension array must be 'decoded' to identify their content. Thus, this review will not cover many microarrays used for gene expression analysis made by ink jet or contact printing since spot sizes are typically larger than 50 μm. Instead, we will focus primarily on ensembles with nanometer-sized elements as well as directed and randomly ordered arrays with sub-30 μm sized features.

2. Ensembles

2.1. Electrical Ensembles

The definition of an ensemble is a group of identical elements that are addressed in unison. This definition arose from electrode ensembles in which a collection of electrodes shares a common electrical connection. Nanoelectrode ensembles (NEEs) were pioneered by Martin and co-workers over 20 years ago.[5] Motivated by the unique diffusional properties of nanoscale electrodes, they invented a technique, now known as template synthesis, to quickly and reproducibly create millions of nanoscale electrodes by depositing metals inside nanoporous membranes. NEEs created in templates can have densities upward of 10^{11} electrodes/cm^2, easily putting them in the very high density category.[6]

Before NEEs were created, there was considerable interest within the electrochemical community in experimentally validating the diffusion properties of ions as the size of electrodes decrease and approach the dimensions of the electric double layer.[7,8] Models predicted substantially higher mass transfer rates in microelectrodes due to radial diffusion, which would enable ultrafast electrochemical measurements, compared to measurements using bulk electrodes that operate via planar diffusion.[9,10] Smaller electrode sizes also promised access to microenvironments not accessible to larger electrodes, such as cells. The ability to make measurements in this realm drove researchers to taper microelectrodes to smaller and smaller sizes. A persistent issue that arose, however, was the decreasing current as electrodes shrank. NEEs successfully addressed both the issue of decreasing electrode size, by using nanoporous templates, and the issue of increasing the overall current, by multiplexing the nanoelectrodes.[11]

The diffusional properties of NEEs are influenced by the nanoelectrode density and voltage scan rate of the experiment.[12] If the electrodes are tightly packed and the scan rate is relatively slow, then their individual radial diffusion profiles overlap, resulting in planar diffusion (Figure 1). In this 'total overlap' regime, the NEE will respond similar to bulk electrodes during cyclic voltammetry (CV) measurements, except with a lower background signal. Microelectrodes spaced far apart and scanned quickly maintain radial diffusion and show a characteristic sigmoidal CV trace. The ideal case is to have the electrodes at an intermediate density to maintain radial diffusion while using the electrode area as efficiently as possible.[13] Many researchers have used the condition (C1)

$$R_0 > 6R_b, \text{ (C1)}$$

where R_0 is one-half the interelectrode distance and R_b is the electrode radius (Figure 1b), as a guide to designing arrays for the ideal case. This equation, which can be traced

Table 1. Comparison of Microelectrode Radius with Its Diffusion Zone Radius Comparison of Microelectrode Radius, R_b, with the Simulated Critical Domain Radius, R_0^c, and the Diffusion Radius Obtained from C1[a]

R_b (μm)	R_0^c (μm)	R_0^{C1} (μm)
10	50	60
1	34	6
0.1	15	0.6
0.01	5	0.06

[a] The formal definition of R_0^c is defined in ref 9, but for our purposes here it can be considered as one-half the minimum distance between electrodes that avoids significant overlap of their diffusion profiles. Adapted with permission from ref 13. Copyright 2005 Elsevier B.V.

back to work by Saito in 1968,[14] is accurate for moderately sized electrodes, near 10 μm in radius, but more recent models predict it underestimates the size of the diffusion zone from smaller electrodes.[13] The recent simulations by Compton and co-workers could not be simplified by a single equation, but results are given in Table 1 for electrodes whose sizes vary over 4 orders of magnitude. Using varying densities and sizes, electrode ensembles operating in both 'total overlap' and 'radial' diffusion modes have been successfully used in chemical sensing.[15,16]

2.1.1. Fabrication

Several methods now exist to create NEEs, including methods based on self-assembly,[17,18] but the most commonly used techniques are based on the template methods of Martin and co-workers.[5,19,20] In these methods, the template is either an anodized alumina membrane or a polycarbonate track-etch membrane. The anodized alumina is created electrochemically in a two-step process starting from Al foil. By varying time, anodization potential, and the electrolyte solution composition, pores of different length and diameter can be made.[21−23] Unlike track-etch membranes, alumina membranes can be created using equipment readily available in an electrochemistry lab. Track-etch membranes are created by exposing thin polymer films to nuclear fission fragments in the chamber of a nuclear reactor. These subatomic particles tear through the film, leaving straight nanometer-size tracks that can be chemically amplified by etching to create monodispersed pores with controlled diameters.[24] Both types of membrane are commercially available with pore sizes between 10 nm and 10 μm and densities over the range from 10^4 to 10^{11} pores/cm^2.

Templates are typically filled either by electrodeposition or electroless deposition. During electrodeposition, one side of the membrane is sputter coated with a metal that serves as an electrode and then used to electrodeposit additional metal from an electroplating solution in contact with the open pores on the opposite side of the membrane.[25] This versatile method can be used to deposit both metals and conducting polymers.[26] Electroless deposition is performed by sensitizing the pores with Sn^{2+} and then using the physisorbed Sn^{2+} to electrolessly reduce ammoniacal $Ag(NO_3)$.[15] The silver nanoparticle seeds then catalyze electroless deposition of other metals, such as gold, which grows inward from the pore walls. Thus, metal tubules are electrolessly grown until they become solid cylinders. Along with these two methods, other filling mechanisms have also been demonstrated such as chemical polymerization,[27] sol−gel deposition,[28] and chemical vapor deposition (CVD).[29]

Alumina and track-etch membranes have also been used for a number of alternative applications besides NEEs. For example, they have been used as stencil masks to etch an array of wells[30−32] or deposit materials in a geometry dictated by the pore locations.[33] The filling material is not exclusive to metals and polymers; carbon,[34,35] semiconductors,[36] and Li^+-intercalation materials[37−39] have also been prepared. Carbon nanotubes (CNTs) deposited in alumina membranes have been used as IR detectors,[40] and electrodeposited Ge nanowires have been used as photoresistors.[41] The pores can also be used to synthesize nanomaterials, such as tubules and wires, that can be released by dissolving the membrane.[42,43] While these alternative technologies have not yet been used in chemical sensing ensembles, their common starting point of a very high density template makes them noteworthy.

2.1.2. Applications

The first chemical sensing application of NEEs took advantage of their increased diffusion rates, demonstrating a lower detection limit for several standard electrochemical species such as $Ru(NH_3)_6^{3+/2+}$, $Mo(CN)_8^{4-/3-}$, and $TMAFc^{1+/2+}$ ([(trimethylamino)methyl]ferrocene).[15,44] The detection limit in a voltammetric experiment is dependent on the ratio of analytical signal to background (S/B). Signal is caused by Faradaic current that occurs at the electrode during the redox reaction of the analyte.[45] In a NEE, at appropriately high scan rates, the signal can be as high as macroelectrodes due to the radial diffusion zone around each nanoelectrode and the large number of electrodes in the ensemble. Background is predominantly caused by a double-layer charging current at the electrode−solution interface and proportional to the area of the conductive portion of the electrode. For most electrodes, the conductive area is equal to the total area, but for NEEs the conductive area is only about 0.1% of the entire electrode surface. Therefore, since the signal is the same but the background is several orders of magnitude lower, the S/B for a NEE is significantly higher than for conventional electrodes.

Other groups have used this increase in S/B to detect more interesting electrochemically active species using NEEs. Ugo and co-workers, for example, utilized NEEs to detect submicromolar concentrations of iodide and cytochrome *c* (cyt *c*).[46] The iodide concentration in table salt was measured using CV with a detection limit more than 10 times lower compared to a bulk electrode. Cyt *c* was of particular interest because electrochemical studies of cyt *c* usually require a promoter or mediator to avoid electrode poisoning due to adsorption. The high sensitivity of the NEE and differential pulsed voltammetry method used enabled the concentration of the cyt *c* to be reduced low enough to avoid poisoning, thereby allowing detection without a promoter.

Recently, several groups have used very high density ensembles to electrically detect DNA hybridization events. Kelley and co-workers used NEEs to electrically detect DNA hybridization. The NEEs were made by electroless deposition of gold into polycarbonate track-etch membranes. The polycarbonate membranes of these standard 2-D NEEs were then O_2 plasma etched to yield 3-D brush-like electrodes.[47] This change in geometry allowed more DNA to bind to each electrode, decreasing the NEEs detection limit into the attomole range.[48] DNA hybridization was measured by CV using $Ru(NH_3)_6^{3+}$ and $Fe(CN)_6^{-3}$. Ru(III) was reduced to Ru(II) by electron transfer through dsDNA, which was formed by the hybridization of target ssDNA to self-assembled ssDNA probes on the electrode surface (Figure

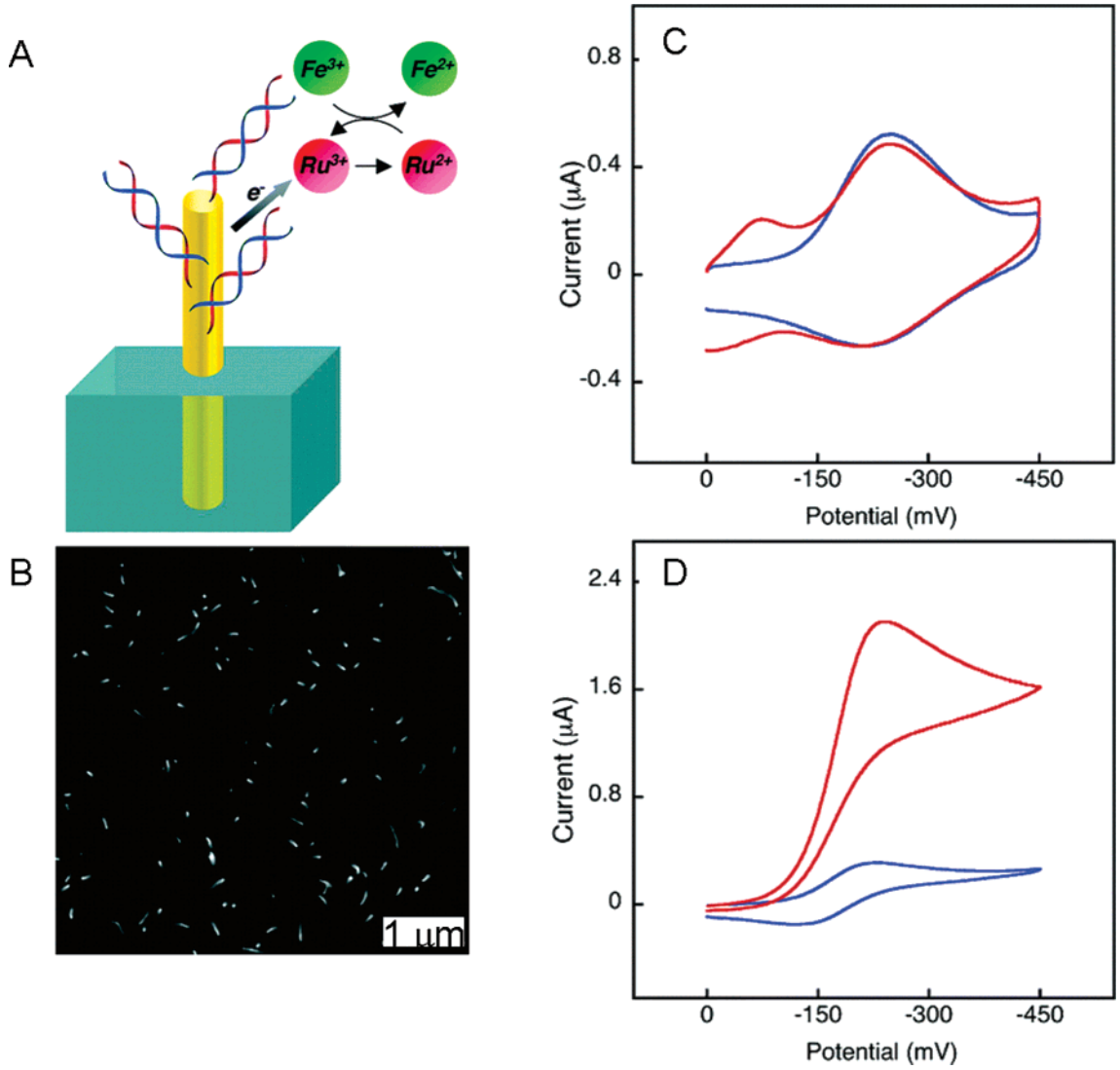

Figure 2. (A) Schematic of Ru(III)/Fe(III) electrocatalysis at a DNA-modified Au NEE. (B) Scanning electron micrograph of a NEE. The white spots are the tips of the Au nanowires protruding the polycarbonate membrane. The individual wires extend ~200 ± 10 nm from the membrane surface. Representative cyclic voltammograms for an 18-mer duplex DNA-modified bulk (C) Au electrode and (D) NEE. Solutions contain 40 μM $Ru(NH_3)_6^{3+}$ and 0 (blue) and 32 μM (red) $Fe(CN)_6^{-3}$. Scan rate for all CV experiments was 100 mV/s. Background subtraction was performed so that all scans could be directly compared. Reprinted with permission from ref 48. Copyright 2005 American Chemical Society.

2). Ru(III) was catalytically regenerated from Ru(II) by conversion of excess of Fe(II) to Fe(III) in solution, which amplifies the response by a factor greater than 10.[49]

Another method of DNA detection has been demonstrated by Andreu et al. using a gold nanowire ensemble produced using an anodized alumina membrane.[50] After electrodepositing Au wires in the membrane, the alumina template was dissolved leaving a high surface area Au electrode. Probes of ssDNA were self-assembled onto the electrode, and the surface charge was measured by chronocoulometry using $Ru(NH_3)_6^{3+}$ as a redox marker. The measurement was repeated after hybridization to target DNA, which caused an increase in the surface charge. The detection limit has not yet been determined for this method, but the authors report a 25 bp sequence was detected at micromolar concentrations.[50]

Meyyappan and co-workers also demonstrated DNA detection with NEEs; however, they used a different fabrication method to create a NEE composed of multiwalled carbon nanotubes (MWCNTs). The MWCNTs were grown on a lithographed Si wafer from patterned Ni catalyst spots using plasma-enhanced chemical vapor deposition (PECVD).[51] The nanotubes were nominally 5 μm in length and 80 nm in diameter with a density of 2×10^9 nanotubes/cm^2. The wafer and MWCNTs were then coated by CVD with an insulating layer of SiO_2, which was later polished to expose the nanotube tips. These tips were electrochemically etched, leaving hydroxyl and carboxylic acids groups that could be used to covalently bind analytes such as DNA. DNA hybridization was detected using the catalytic redox species tris(2,2′-bipyridyl)ruthenium(II), $Ru(bpy)_3^{2+}$, to oxidize guanine residues in dsDNA. Using AC voltammetry and an 18 bp probe sequence, 300 bp PCR amplicon targets were detected with sensitivity approaching that of laser-based fluorescence techniques.[52]

Very high density ensembles have also been made without photolithography or template methods. Walt and co-workers demonstrated a method of creating electrode ensembles starting from a fiber optic bundle with a density higher than 10^6 fibers/cm^2.[53] The cladding of a fiber optic bundle was etched anisotropically, resulting in pointed fiber optic cores that were then sputter coated with gold. This bulk gold surface was then covered with an insulating paint, leaving

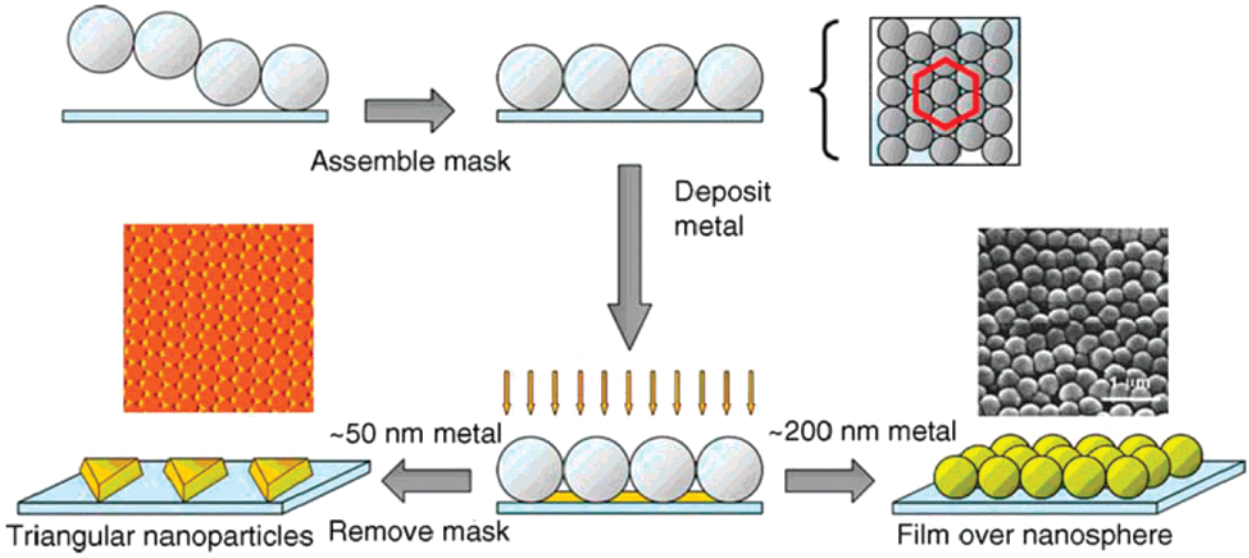

Figure 3. Illustration of patterning by nanosphere lithography (NSL). A colloidal monolayer is created and used as a mask for metal deposition in the voids between the nanospheres. Deposition of ~50 nm of metal followed by mask removal creates a triangular nanoparticle ensemble useful for LSPR. Deposition of ~200 nm of metal results in a textured metallic film used in SERS studies. Reprinted with permission from ref 61. Copyright 2005 Elsevier B.V.

~1 μm diameter Au tips periodically protruding the insulation. The fiber optic bundles were used as electrode ensembles to optically detect the electrogenerated chemiluminescence signal from $Ru(bpy)_3^{2+}$ and tripropylamine in phosphate buffer.[53] In a method analogous to the insulated fiber optic tips, Lowe et al. showed that an ensemble of conical CNTs grown on a Pt electrode could be partially insulated to create a NEE as demonstrated by sigmoidal CV traces showing steady-state diffusion, a characteristic of NEEs.[54]

Very high density ensembles, characterized by their bulk addressability, have proven useful in electroanalytical chemistry, especially for the measurement of DNA hybridization. Inspired by the diffusion properties of ever smaller microelectrodes, the template methods developed by Martin to create NEEs have led to numerous devices with improved S/B ratios and lower limits of detection.

2.2. Optical Ensembles

Metal nanoparticle ensembles have also been used for optical sensing. Metal nanoparticles and thin films have distinct optical properties due to surface plasmon resonance (SPR), which is a collective oscillation of surface electrons excited by electromagnetic radiation. Radiation impinging on a thin metal surface can excite the surface electrons into a propagating wave known as a surface plasmon polariton. A similar oscillation occurs in nanoparticles, and this phenomenon is called localized surface plasmon resonance (LSPR) because it is confined to the surface of isolated particles.[55] In both cases, the resonant frequency depends on the dielectric constant of the surrounding material and in the case of the LSPR it also depends on the size and shape of the nanoparticles. Islands of metal nanoparticles that have been functionalized with capture probes have been used as sensors.[56] Wavelength-shift LSPR sensors can detect analyte binding because the act of binding changes the dielectric constant near the surface of the film, and therefore, the resonant wavelength also changes. Van Duyne and coworkers pioneered nanosphere lithography (NSL)[57] to make nanoparticle arrays for LSPR sensors, but other methods also exist.[58,59] NSL uses hexagonally packed polymer nanospheres on a glass surface to create a stencil mask. Depositing metal onto this monolayer results in small, 20−1000 nm, metallic triangles in the voids between the spheres (Figure 3).[60] An LSPR sensing substrate results after removing the spheres, leaving a homogeneous ensemble of uniform metal triangles, the size and shape of which can be tuned. Deposition of a thicker film onto the spheres results in a highly textured metal surface, which is useful for surface-enhanced Raman scattering (SERS).[61] SERS surfaces can enhance the Raman effect by ~10^6. This enhancement is caused in part by the local electromagnetic field resulting from LSPR, which then induces a dipole in molecules that are in proximity (<4 nm) to the metal surface, thereby raising the effective Raman cross-section of the molecule.[61] SERS surfaces have also been used as sensors by measuring the Raman spectrum of analytes bound to patterned substrates.[62] Both LSPR and SERS substrates have been used for sensing in either transmissive or reflective modes, and in both cases the signal originates from the entire ensemble.

Wavelength-shift LSPR sensing has been used to detect several biomolecules including proteins, DNA, and the biomarker for Alzheimer's disease, amyloid-beta-derived diffusible ligand (ADDL). The carbohydrate-binding protein concanavalin A (con A) was one of the earliest analytes detected using LSPR by exposure to a mannose-coated Ag pattern made by NSL.[63] Binding of 0.19 μM con A could be monitored in real time by tracking the resonant wavelength. A slightly modified platform was used for DNA detection, consisting of Au-coated silica nanoparticles on top of a Au-coated glass slide. Peptide nucleic acid (PNA) bound probes were able to detect as little as 0.677 pM complementary DNA.[64] This platform was also used for immunoassays by attaching protein A to the Au-coated silica beads and then using protein A to bind C-reactive protein, fibrinogen, and immunoglobulins IgA, IgD, IgG, and IgM.[65] These six proteins were spotted to create a low density array that was able to detect 100 pg/mL of antigen by wavelength-shift LSPR. The biomarker ADDL was measured in the cerebrospinal fluid of Alzheimer's patients in a LSPR sandwich assay.[66] After ADDL bound to the nanoparticle

ensemble, a resonant wavelength shift of 28.5 nm was observed, with an additional shift of 15.4 nm being measured after binding of the secondary antibody. Compared to the control sample, with shifts of 2.9 and 4.3 nm respectively, the biomarker was readily identified.

SERS ensembles have been used to detect glucose, viruses, and warfare agent simulants. Using a mixed monolayer of hydrophilic and hydrophobic groups on a SERS substrate, glucose has been detected both in vivo and in vitro. This real-time sensing measured glucose using its spectral signature rather than indirectly, as in most electrochemical sensors.[67] Antibody-captured feline calicivirus particles on a gold substrate were detected in a sandwich assay by attaching Au nanoparticles coated with a Raman-active reporter molecule.[68] Virus concentrations as low as 10^6/mL could be detected. The anthrax biomarker calcium dipicolinate (CaDPA) has been detected in the spores of *B. subtilis*, which is *B. anthracis* simulant.[69,70] An infectious dose is 10^4 spores and as few as 1400 spores could be detected using the SERS platform. Likewise, a mustard gas simulant was also detected well below the harmful limit. This measurement was performed on a portable Raman spectrometer, enabling measurements in the field. Tan and Vo-Dinh also report a field deployable SERS spectrometer, which has been used to detect simulants for warfare agents such as sarin, soman, tabun, and sulfur mustard (HD).[71]

Ensemble sensors probed optically have also been made from hydrogels. A colloidal crystal, made of 100-nm diameter polymer spheres, has been coated in a hydrogel that is responsive to heavy metal ions and glucose.[72] Upon exposure to analyte, the hydrogel swells changing the lattice spacing of the crystal, which is measured by the change in the diffraction pattern of the crystal. Similarly, the swelling of microlens made of hydrogels can be monitored by measuring their change in focal length.[73] These microlenses were demonstrated by detecting antibody−antigen binding.[74]

3. Very High Density Arrays

3.1. Directed Arrays

3.1.1. Photolithography

Arrays that contain elements whose identity is purposefully mapped to specific positions are known as directed arrays. In order to create very high density directed arrays, photolithography is used, sometimes in conjunction with electron-beam or soft lithography. Photolithography is the workhorse of the microelectronics industry and used to pattern intricate circuits on the micrometer and submicrometer scales with feature sizes below 100 nm. Using UV radiation and photomasks, photolithography patterns light-sensitive resists atop semiconducting or insulating substrates. The developed photoresist protects the underlying chip in specific regions for subsequent processing steps, such as etching, coating, or doping. Complex circuits, such as microprocessors and memory, are created by repeated cycles of protecting and processing. These techniques of photoprotecting/deprotecting have also been used for rapid parallel chemical synthesis, as will be described below.

Electronic devices that consist of an array of components, such as the array of capacitors that make up dynamic random access memory (DRAM), can have densities >100 000 per mm^2. Many other microelectronic arrays also have very high densities, including charge-coupled devices (CCDs) and complementary metal−oxide−semiconductor (CMOS) sensors. These detectors can reach several megapixel resolution on chips smaller than 1 cm^2 and be manufactured at modest cost. A digital micromirror device (DMD) is a dense array of actuatable mirrors about 10 μm on a side. DMDs are finding application in photolithography as dynamic replacements for photomasks in addition to their use in displays. Spatial light modulators (SLMs), which use an array of liquid crystals pixels, can also modulate light in two dimensions. While these four microelectronic devices have not yet been used directly as transducers for chemical sensing, they are widely used for spatial control of chemical processes (DMD and SLM) and capturing spectroscopic data and images (CCD and CMOS).

Photolithography can also be used to fabricate arrays of chemically sensitive field effect transistors (CHEMFETs).[116] Over their 35 year history, CHEMFETs have been used to detect several analytes, including K^+,[117] Na^+,[118] urea,[119] enzymes,[120,121] and DNA.[122,123] CHEMFETs can, in principle, be arrayed at high density, enabling multiplexed detection; however, there are very few examples of densely arrayed CHEMFETs in the literature.[124,125] Recent advances in nanoparticle synthesis have enabled the creation of semiconducting nanowires, such as silicon nanowires (SiNWs) and carbon nanotubes (CNTs), that can be used as the channel material in place of bulk semiconducting crystals. There are many reports of SiNW- and CNT-FET sensors, including several good reviews.[125,127,128,267] There are also some papers that are critical of the feasibility and selectivity of these devices.[134,268−273] The most common analytes detected up to now include small cations, such as H^+ and Ca^{2+},[129] and biomolecules such as DNA and antigens.[135,136,138−144] These nanowire channels typically have dimensions of tens of nanometers in diameter and several microns in length. This <1 μm^2 footprint makes these devices capable of very high density arrays; however, nanowire FETs have thus far been arrayed with densities of only ~50 FETs/mm^2.[143] For this reason, a detailed description of these arrays is beyond our scope.

3.1.2. Dip-Pen Nanolithography

Since the 1980s, there has been a push to extend photolithography beyond the scope of electronics and use its microscale patterning capability to create sensing devices.[75] Some of the first microscopic devices made were cantilevers for use in scanning probe microscopies, such as scanning tunneling microscopy (STM) and atomic force microscopy (AFM). Cantilevers, usually comprised of silicon, can be made in a variety of shapes and sizes but are typically ~100 μm long, 10 μm wide, and 2 μm thick. Cantilevers are also used in dip-pen nanolithography (DPN),[76,77] which is an adaptation of AFM. DPN uses cantilevers with atomically sharp tips to pattern 'inks' onto substrates. Following the first demonstration of using DPN to pattern alkanethiol inks on gold substrates,[78] various other materials, including polymers,[79] proteins,[80] peptides,[81] and sols,[82] have been patterned on metallic, semiconducting, and insulating substrates. Patterned feature sizes are approximately 100 nm wide and have been made as small as 15 nm.[83]

DPN has enabled the creation of very dense sensing arrays. Protein arrays of rabbit immunoglobulin gamma (IgG) and lysozyme have been patterned directly by DPN and shown to retain their biomolecule recognition capabilities.[84] To avoid denaturing the proteins, the cantilever tips have been modified with a hydrophilic monolayer, such as 2-[meth-

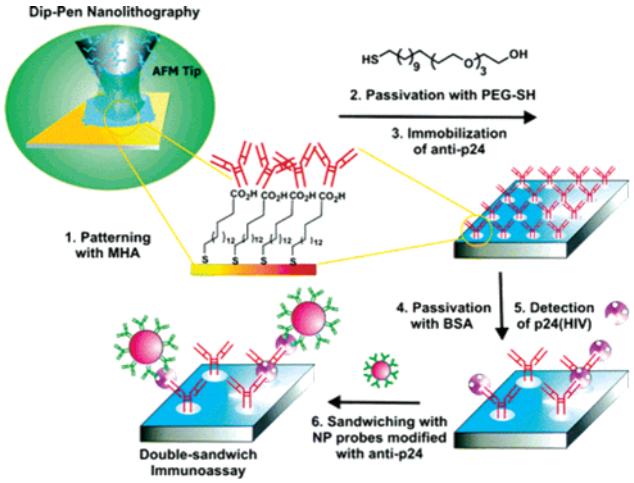

Figure 4. Schematic representation of the sandwich immunoassay format used to detect HIV-1 p24 antigen with an anti-p24 antibody nanoarray made by DPN. The HIV-1 p24 antigen was sandwiched between anti-p24 antibody bound to the MHA patterned surface and gold nanoparticle probes coated with anti-p24 antibody. The change in height due to the nanoparticle binding event could be detected by AFM. Reprinted with permission from ref 86. Copyright 2004 American Chemical Society.

oxypoly(ethyleneoxy)propyl]trimethoxysilane, and maintained at 60−90% relative humidity during patterning. IgG has also been arrayed indirectly by patterning 16-mercaptohexadecanoic acid (MHA) on a gold substrate. The patterned MHA then selectively binds IgG.[85] This strategy was used in a sandwich immunoassay for detection of human immunodeficiency virus type 1 (HIV-1) as shown in Figure 4.[86]

Nanoparticle binding has also been used for oligonucleotide detection by patterning the ssDNA using DPN and exposing this array to gold nanoparticles labeled with the complementary DNA strand.[87] Thus far, arrays made by DPN have only been fabricated for the detection of two analytes,[88] although the technique could potentially be applied to massively parallel multiplexed detection. A major step toward this goal has already been taken by Mirkin and co-workers with their creation of a cantilever array containing 55 000 cantilevers in a 1 cm^2 array (Figure 5).[76,89,90] This array has been used to pattern 88 000 000 gold dots, each 100 nm in diameter, and will undoubtedly be used for highly multiplexed sensing in the future.

3.1.3. Chemical Synthesis by Photolithography

In 1991, Fodor and co-workers pioneered the application of photolithography to combinatorial chemical synthesis to create very high density biomolecule arrays.[91] The starting point for an oligonucleotide array is a quartz substrate modified with photochemically removable protecting groups.[92,93] Areas of the substrate are then activated by exposure to UV radiation through a photomask. Next, the substrate is incubated with hydroxyl-protected deoxynucleosides, which results in addition of the first base to the activated areas. A different mask is then used to expose and deprotect other regions of the substrate, enabling those areas to react with the next protected deoxynucleoside. The process of deprotection and reaction is repeated resulting in the synthesis of different oligonucleotides in different locations on the array (Figure 6). All 4^n combinations of an n-mer oligonucleotide can be synthesized in $4 \times n$ steps. Oligonucleotides synthesized photolithographically are generally less than 30

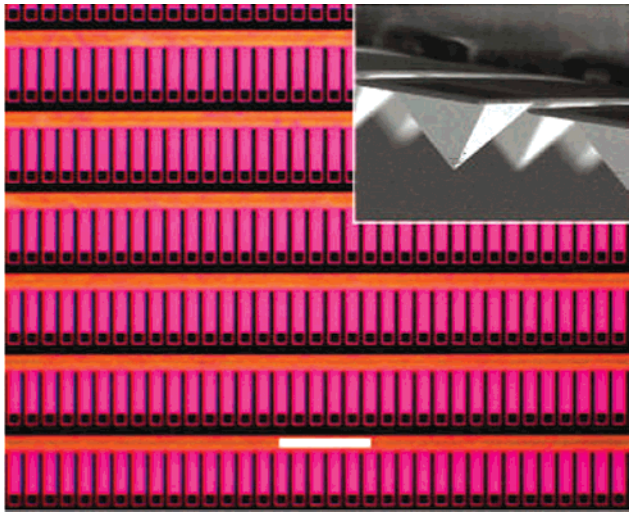

Figure 5. Optical micrograph of a small section of a DPN array containing 55 000 cantilevers. Scale bar = 100 μm. (Inset) Electron micrograph of the cantilever tips. Reprinted with permission from *Nature* (http://nature.com), ref 76. Copyright 2004 Nature Publishing Group.

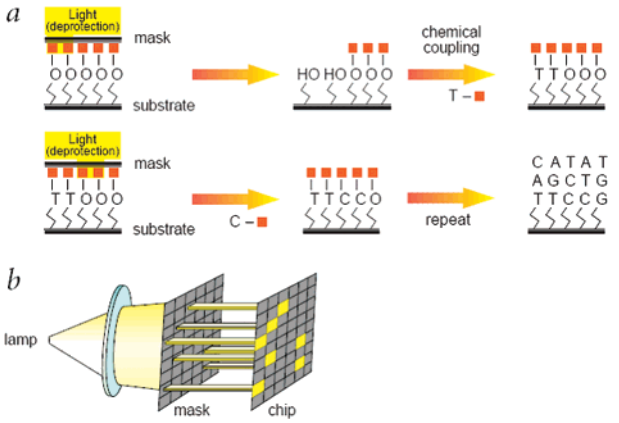

Figure 6. (A) Light-directed oligonucleotide synthesis. A substrate coated with a covalently bound linker molecule containing a photolabile protecting group (orange squares) is locally exposed to light through a photomask. The exposed regions are deprotected and then reacted with protected nucleotides. The process is repeated, deprotecting and reacting different sites with different nucleotides, to synthesize arbitrary DNA probes at each site. (B) Schematic illustration of a photomask used to expose an array. Reprinted with permission from *Nature* (http://nature.com), ref 99. Copyright 1999 Nature Publishing Group.

bases long with densities >250 000 features/cm^2.[4] While feature size is usually about 20 μm on edge, features as small as 8 μm have been demonstrated.[94] One of the drawbacks of this fabrication technique is the need for possibly 100 photomasks to create the desired array of sequences.[95] Patterning the light using a DMD, in place of photomasks, is one method to alleviate this problem.[96−98] Feature sizes as low as 4 μm have been reported using DMDs to pattern oligonucleotides.[96]

Oligonucleotide arrays have been used for gene expression and genotyping.[99] Genes are expressed in cells by first translating genomic DNA into messenger RNA (mRNA) followed by transcription of mRNA into functional proteins. To test for expressed genes in a sample, typically mRNA is reverse transcribed into complementary DNA (cDNA) containing a fluorescent label. The cDNA is more stable than RNA and can also be amplified with polymerase chain

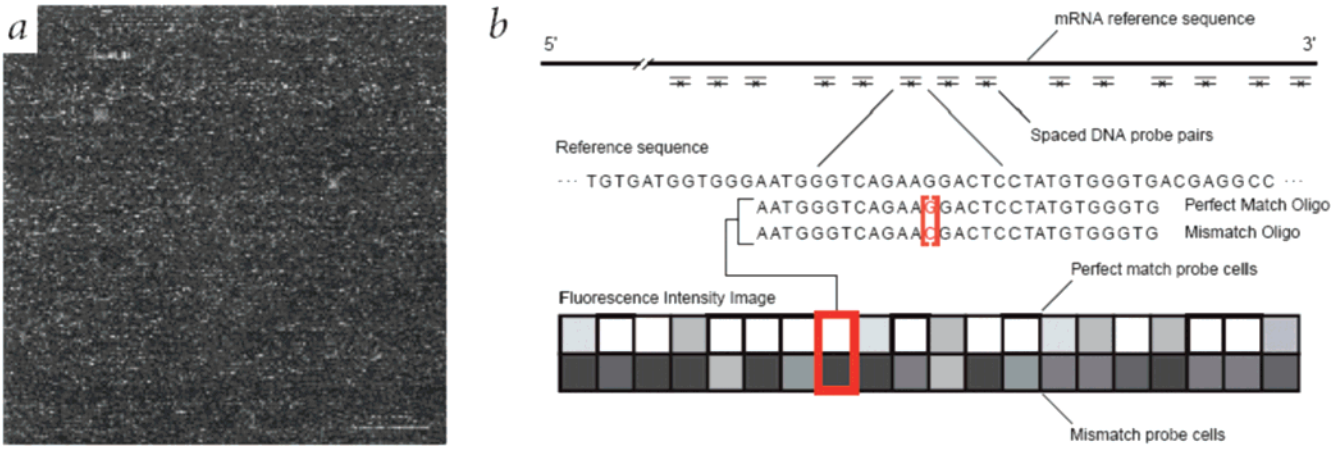

Figure 7. (A) Gene expression monitoring using an array containing 40 000 human genes and expressed sequence tags. The optical micrograph shows a substrate, 1.28 × 1.28 cm, containing features less than 22 × 22 μm. (B) The oligonucleotide probes are chosen based on composition design rules and a uniqueness criterion. Use of perfect match (PM) and mismatched (MM) probes greatly reduces background and cross-hybridization signals, increasing accuracy and reproducibility. Reprinted with permission from *Nature* (http://nature.com), ref 99. Copyright 1999 Nature Publishing Group.

reaction (PCR). Alternatively, the mRNA can be fluorescently labeled and then randomly fragmented into 50−100 bp segments and hybridized to the array. The array contains thousands of 25-mer oligonucleotides sequences, called probes, known to be complementary to genes.[100,101] Each gene from a sample, which spans hundreds of bases, is covered on the array using multiple 25-mer sequences. This strategy offers a type of redundancy because while the probe sequences are not the same, several probes encode for the same gene. Expressed genes are identified based on the intensity and location of the fluorescent signal. To quantify nonspecific hybridization and background signals, the perfect match (PM) probes on the array are placed next to mismatch (MM) probes, which are identical to the PM except for one nucleotide in the center of the sequence, which is different (Figure 7).[101] Thus, cross-hybridized signals can be subtracted from the PM signal. This lithographed platform, developed by Affymetrix Inc. under the name GeneChip, has been used for genome-wide expression analysis for over 10 years.[102] The density of this array enables comprehensive analysis of cell functions by monitoring thousands of genes in a sample simultaneously.[102] Gene expression studies are widely used to identify and study diseases, such as cancer, as well as study basic biological functions.[103−106]

Genotyping can also be performed using lithographed arrays. Genotyping refers to identification of genetic differences, such as single-nucleotide polymorphisms (SNPs), which account for phenotypic differences between and within species. A SNP is an alteration in a single nucleotide in genomic sequence that occurs in at least 1% of a population. For example, in the sequence AATTGAT, a SNP of the sequence would be AATCGAT. Theoretically, there are about 11 million known SNPs in the human genome.[107] Genetic variation can affect an individual's response to a disease and environmental factors, such as toxins or drugs. Genotyping will help identify genetic disease markers and accelerate new therapies. SNPs can be identified using two probe sequences that vary in only one position. The probe that forms the most stable duplex will result in the highest fluorescent signal and identify which allele is present in the sample. On the GeneChip platform, a single SNP is queried with 40 probes. A quartet of four probes represents the PM and MM for both alleles with the SNP position in the center. Two more pairs of quartets, with the SNP position shifted

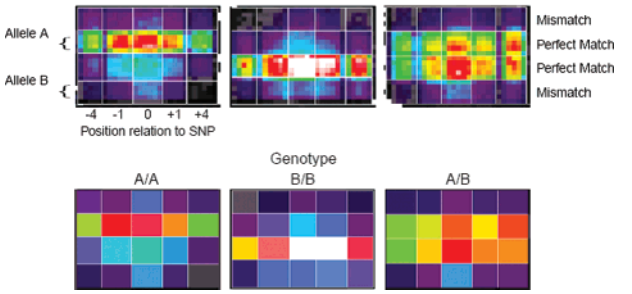

Figure 8. Section of a genotyping array that shows the fluorescence intensity pattern for a set of probes that interrogates a single locus. The upper half of the probe blocks interrogate the A alleles and the lower half interrogate the B alleles. Each half has pairs of probes centered on polymorphic position and offset one and four bases to either side. The pairs consist of a PM and a MM to the reference sequence for the specific allele. The presence of the AA homozygote, the AB heterozygote, and the BB homozygote is shown. Reprinted with permission from *Nature* (http://nature.com), ref 99. Copyright 1999 Nature Publishing Group.

±1, ±4 from the center, make up 20 probes. The remaining 20 probes are the anti-sense version of the first 20 probes (Figure 8).[94,108] Presently Affymetrix arrays can simultaneously detect over 900 000 SNPs. Similar arrays have been used for a broad range of purposes from cancer research to drug development.[109−112]

It is not the purpose of this review to cover the many sophisticated applications of gene chips or DNA microarrays. For a more comprehensive overview of such applications, a number of excellent reviews are available.[113−115] It is important to note here that while the original purpose of DNA microarrays was to use the specificity of hybridization to determine the sequences present in a genetic sample, this approach is no longer the preferred one. Modern genotyping experiments now implement a two-phase approach. In the first phase, a series of complex biochemistry and molecular biology steps is employed to interrogate many different genetic sequences simultaneously and prepare the resulting sample for hybridization to the array. The hybridization step that follows is simply used as a readout for the assay. In several implementations of this two-phase approach, the goal is to interrogate many SNPs in parallel and the strategy is to convert the small single-base differences into molecular signals that allow easy discrimination. To this end, the arrays

rarely need single-base specificity because the assay converts a single-base mismatch into a multiple-base readout difference. More information about this strategy can be found in the section below on Randomly Ordered Arrays.

3.2. Randomly Ordered Arrays

3.2.1. Introduction

A randomly ordered array is classified as such because its elements are randomly self-assembled into a pattern. The identity of a probe at any location in the array is therefore not known a priori. This is fundamentally different than directed arrays, where array elements are synthesized or placed in known locations. A template is used to structure self-assembled arrays. Sensor elements, such as microspheres with different surface chemistries, randomly fill the template to create a multiplexed sensing platform. After identifying the surface chemistry of each element, in a process called registration, analytes are detected based on which array elements they interact with.

Our lab has pioneered the use of fiber optic bundles as templates for randomly ordered array sensors.[146−150] A fiber optic bundle is a collection of individual fiber optic cores that share a common cladding. Each core can act as a waveguide to transmit an optical signal without cross-talk between adjacent fibers. Typically, a fiber bundle contains between 5000 and 50 000 waveguides with individual fibers in the array ranging in diameters between 3 and 7 μm. These bundles are coherent, such that the position of a particular fiber at one end of the bundle corresponds to its position at the other end. The different glass compositions of the core and clad materials cause them to etch at different rates. When treated with an acidic etching solution, the core etches faster than the clad and creates an array of uniform microwells. These femtoliter-sized microwell chambers can then be loaded with a variety of microsensors or probes, living cells, or they can be used to house reactive species, such as enzymes.

For bead-based sensing applications, indicator or probe molecules are covalently attached to polymer or porous silica beads that can then be loaded into the wells. Each bead type is prepared in a separate reaction scheme, and the different bead types are then pooled before loading into the array. The wells are sized to ensure that there is only one bead per well. For most applications, the transduction mechanism is based on fluorescence as it allows for simple optical instrumentation. Detection is performed using a microscope objective to launch excitation light into the proximal end of the fiber and detecting the epi-fluorescence from the beads housed on the distal face of fiber (Figure 9). Parallel detection involving thousands of beads is accomplished using a CCD camera. The platform can be spectrally multiplexed using different combinations of excitation and emission wavelengths (Figure 10).

The fiber optic, randomly ordered, addressable array format has several advantages over traditional patterned microarrays, where elements are preregistered by position. The primary benefit is the ease with which randomly ordered arrays can be created. Directed arrays made by ink jet printing, screen printing, or photolithography typically require several fabrication steps where the probability of fabrication errors increase in proportion to the number of processing steps involved. Bead-based random arrays are quickly produced via self-assembly from a few microliters of bead stock solution, which contains $\sim 10^9$ beads/mL (a dry bead powder contains $\sim 10^{12}$ beads/g). Also, new bead pools can be created from any number of existing stock solutions, allowing flexibility as experimental needs change. High sensor density ($\sim$25 000 mm^{-2}) and small array size ($\sim$1 mm^2) enables the measurement of small sample volumes. The high sensor density enables hundreds, possibly thousands, of duplicate sensor probes, which practically eliminates false positive and false negative results. The signal-to-noise ratio, S/N, also is improved, since S/N is proportional to the square root of the number of samples measured, and there are so many duplicate samples available. Finally, because each bead type is prepared in a batch reaction, all the beads of a particular type have virtually identical properties, minimizing array to array variability.

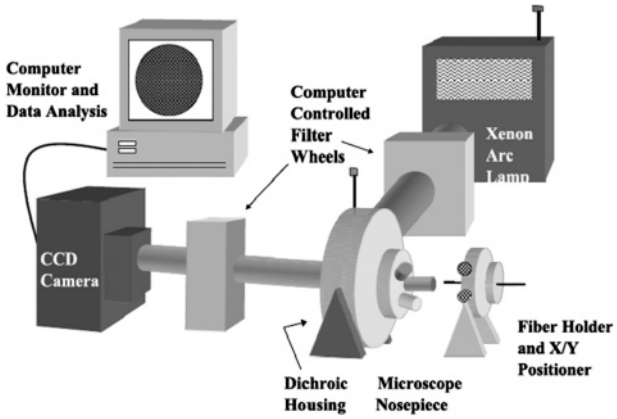

Figure 9. Schematic illustration of a typical epi-fluorescence microscope setup for imaging fiber optic bundle arrays. Reprinted with permission from ref 150. Copyright 2001 Elsevier B.V.

Since the microspheres randomly self-assemble into the wells, a registration process must be performed to map the position of the different bead types after array fabrication. There are two ways array registration can be performed. In one method, beads are encoded by fluorescent dyes, which can be used to identify each bead type and the sensing chemistry they are associated with. Single or multiple fluorescent labels at varying concentrations can be used to create optical barcodes to distinguish multiple bead types.[151,152] These labels must be different from the dyes used during the analytical measurement. Each element of the array can be rapidly decoded using image-processing software. A second class of methods involves using the analytical properties of the chemistries attached to the beads—this approach involves *decoding* the beads. For example, when different DNA sequences are attached to the different bead types comprising an array, the sequences on each bead can be decoded by sequentially hybridizing fluorescently labeled complementary oligonucleotide sequences using a combinatorial algorithm.[153] This method requires that binding is reversible as it is important that the fluorescent DNA be removed in order for the array to be used for analytical purposes. Both registration strategies, optical barcoding and nucleic acid encoding, have been used to encode randomly ordered sensing arrays.

3.2.2. Analyte-Specific Sensing Arrays

Analyte-specific sensors respond with high selectivity to a given species in a lock-and-key configuration. Classic examples of the lock-and-key mechanism include DNA base pairing and antibody−antigen binding. For analyte-specific probes in a randomly ordered array, knowing the specificity

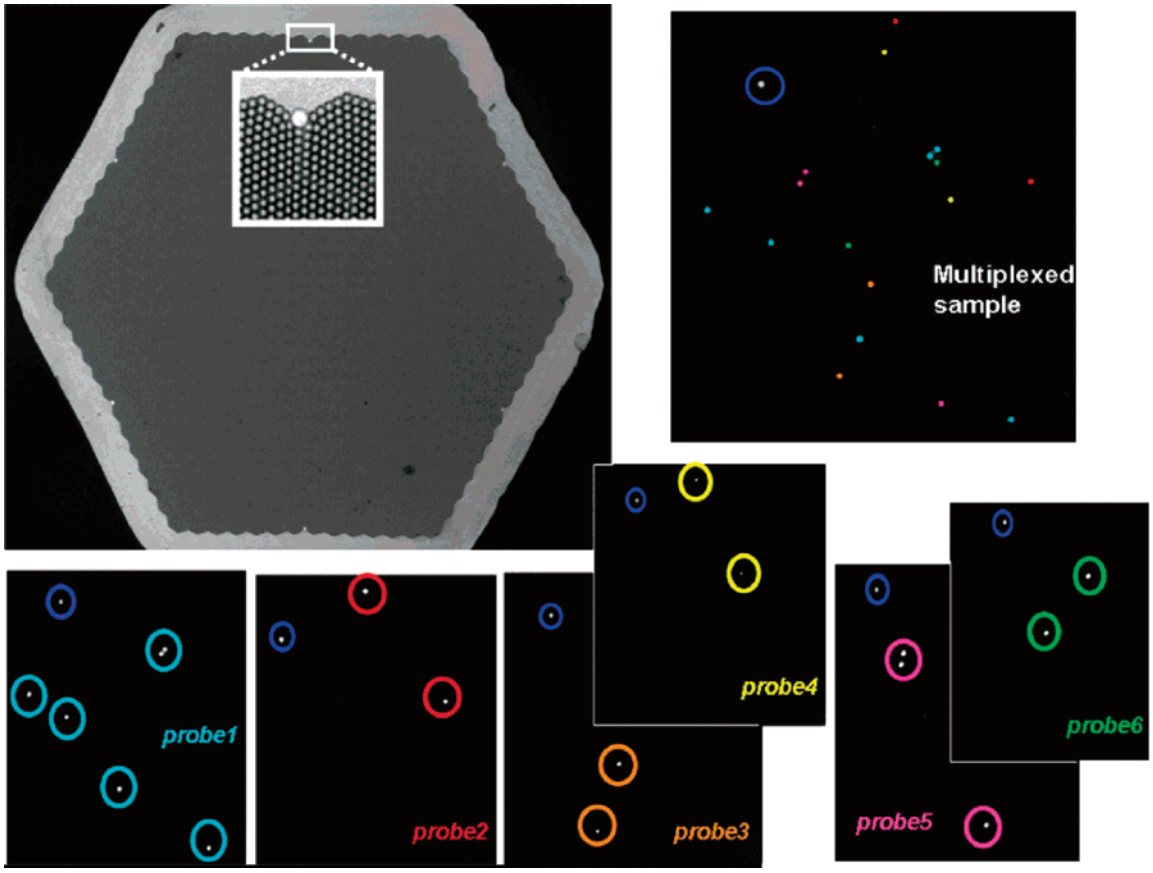

Figure 10. Multiplexed detection using a 1-mm diameter fiber optic bundle containing ~50 000 individual 3-μm optical fibers, each capable of containing an oligonucleotide-functionalized bead. The remaining images show a portion of the fiber bundle and the response of each bead type as well as their collective response. Each bead type is marked using a different color. The blue circle is a positional marker and the same for all images. Reprinted with permission from ref 157. Copyright 2005 American Chemical Society.

of a particular array element is critical for analyte identification. Using optical and nucleic acid encoding strategies, analytes ranging from salivary proteins to biowarfare agents have been detected. The following sections describe randomly ordered arrays used for nucleic acid, protein, and cell-based sensing.

3.2.2.1. Nucleic Acid Detection: Using Optical Barcoding. The optical barcode identification method was demonstrated by Ferguson et al. using 13 different ssDNA probes ranging from 10 to 22 base pairs in length.[151] The beads were encoded using combinations of a Europium dye trapped inside the beads and two externally bound dyes, Cy5 and TAMRA, at different concentrations. Amine-terminated DNA probes were attached to amine-functionalized polymer microspheres using a two-step approach shown in Figure 11. First, the amine functionality of the microspheres was increased by a factor of 10 by coupling polyethyleneimine (PEI) to the bead using glutaraldehyde. Second, the amine-terminated DNA probes were reacted with cyanuric chloride[154] and then covalently bonded to the microspheres. By exciting and monitoring fluorescence at three different optical channels, the concentration of each dye in every bead was determined, thus identifying the ssDNA attached to that bead. Using only 4 μL of solution, target DNA could be detected at concentrations of 100 pM in 10 min and down to 10 fM if allowed to hybridize for longer times (17 h).[151] After analyte detection, the array could be regenerated by dipping the fiber in 90% formamide solution to dehybridize captured targets. The probes were regenerated and reused 100 times with negligible deterioration.

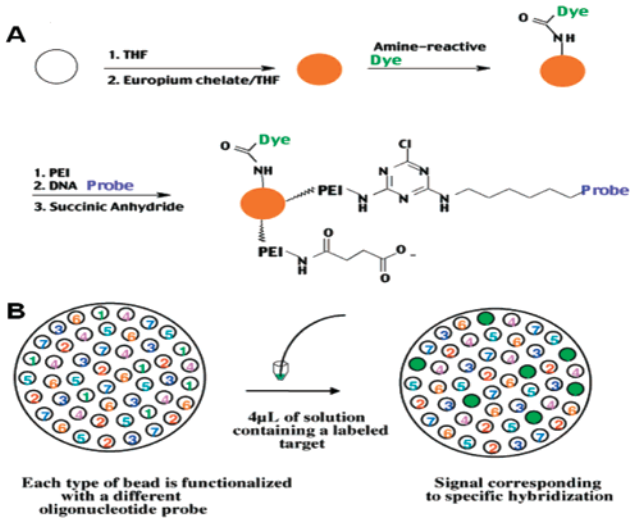

Figure 11. (A) Reaction scheme used to attach encoding dye and probes to microspheres. PEI is used to increase the number of functional groups on the bead surface. (B) Depiction of seven bead types, self-assembled into the wells of an etched fiber optic bundle. Dipping the fiber into labeled target solution produces a response only from the beads with the complementary DNA sequence. Reprinted with permission from ref 151. Copyright 2000 American Chemical Society.

The detection limit of this fiber optic microarray was measured in another experiment, performed under slightly modified conditions. The array was reduced to 3 ssDNA probes about 21 bp long, hybridizations times were fixed at 12 h, and the sample volume was increased to 10 μL.[155] A

smaller number of sensing beads was used, with only ~10 beads of each DNA probe present in the array, in order to concentrate the small number of target molecules. These conditions allowed detection of 100 aM target DNA samples, equivalent to approximately 600 molecules, using a standard white light source, CCD camera, and microscope optics. Another experiment demonstrated 10 aM detection by integrating the fiber array into a microfluidic channel for sample delivery.[156] In the microfluidic system, beads containing two 50-mer oligonucleotide probes were placed in the array and exposed to 50 μL of fluorescently labeled analyte at a flow rate of 1 μL/min.

Fluorescently labeled targets have been used in microsphere arrays for the detection of biowarfare agents (BWAs) and bacterial typing. Six BWAs, including *B. anthracis* and *C. botulinum*, were detected using 50-mer species-specific probes bound to polymer beads. Cy3-modified reverse primers were used to PCR amplify autoclaved samples of BWAs.[154] Using a multiplexed array, these fluorescently labeled targets could then be detected at 10 fM concentrations after 30 min of hybridization using only 50 μL of sample. Twelve strains of the bacteria *E. coli* have also been typed using a similar detection scheme.[157] Fluorescein-labeled reverse PCR primers were used to amplify specific polymorphic regions between 100 and 250 bp in size. Six probe sequences, 33−46 bp long, were each designed to hybridize to a single allele at different polymorphic loci. In principle, these six probes should be able to distinguish $2^6 = 64$ strains in a binary response format; however, due to allele overlaps, only 12 strains were demonstrated.

Detection of unlabeled targets has also been shown using molecular beacon probes. Molecular beacons (MB) are hairpin-shaped oligonucleotides with one end terminated by a fluorophore and the other by a fluorescence quencher.[158] Upon binding of the hairpin section to a target sequence, the fluorophore and quencher separate significantly increasing the fluorescence. Biotinylated MB probes for three different genes were bound to streptavidin-coated beads and used to detect unlabeled cystic fibrosis related targets in a random array. The beads contained a unique concentration of internal encoding dye, but all MB probes used the same fluorophore−fluorescein and quencher−4-(4-dimethylaminophenylazo) benzoic acid.

Randomly ordered microsphere arrays have also been used for multiplexed sandwich assays to detect other dangerous pathogens, such as foodborne bacteria and harmful algae blooms (HABs). The foodborne pathogen *Salmonella* spp. was detected in concentrations between 10^3 and 10^4 cfu/mL.[159] These samples did not require fluorescent labeling and consisted of chromosomal DNA extracted from lysed cells that had been treated with RNase. Microspheres in the array contained six capture probes, between 20 and 35 bp in length, specific to five different virulence genes of *Salmonella* spp. After hybridization of the chromosomal DNA, fluorescently labeled oligonucleotide signal probes complementary to a second site on the bound DNA were added. Use of two hybridization events in this sandwich assay format was hypothesized to increase specificity. This system could accurately detect *Salmonella* spp. even in a mixture of genealogically close organisms, such as *E. coli*, in 1 h. The same basic scheme was also used in the detection of HABs, such as *Alexandrium fundyense*, which are associated with toxic blooms in the Gulf of Maine.[160] The HAB measurements relied on ribosomal RNA (rRNA) instead of DNA for detection but still incorporated sequence-specific capture and signal probes. rRNA is present in thousands of copies per cell and therefore requires no amplification. As few as five cells of HAB were detected without any amplification in 45 min, even in the presence of three other closely related HAB strains. This rapid and specific detection mechanism requires minimal sample processing and should be broadly applicable to a number of pathogenic species.

3.2.2.2. Nucleic Acid Detection: Using Nucleic Acid Encoding. Fluorescent barcoding is limited to the number of distinct optical signatures that can be distinguished. Epstein and co-workers sought to increase the number of different bead types in an array using a combinatorial decoding scheme in which the oligonucleotides attached to the bead were used as an intrinsic identifier.[161] This approach could also be used as a method for sequencing oligonucleotides attached to beads.

Gunderson et al. also demonstrated a combinatorial nucleic acid decoding method.[153] This strategy identifies bead location based on sequential hybridization to known, fluorescently labeled targets. They showed that 1520 bead types, each labeled with a unique oligonucleotide between 22 and 24 bases long, could be identified in only eight hydridization−dehybridization cycles. Three possible fluorescent states (red, green, or neither) were prepared for all 1520 complementary strands and pooled in eight combinatorial groups. This procedure gives $3^8 = 6561$ unique fluorescent responses for all eight pools, more than enough to decode the 1520 sequences. Using a redundancy of about 30 duplicate beads per fiber, this decoding strategy was able to identify nearly 50 000 beads with an error rate of $<1 \times 10^{-4}$ per bead.

The fiber optic random array combined with the nucleic acid decoding strategy of Gunderson et al. has been commercialized by Illumina Inc. and used to study gene expression and genome-wide SNP genotyping. Gene expression and RNA profiling studies have been performed by direct hybridization[162] and DASL[163] (cDNA-mediated annealing, selection, extension and ligation), respectively (Figure 12). Direct hybridization is a standard method for analyzing intact RNA using oligonucleotide probes concatenated to decoding sequences on microspheres. On the basis of the work of Eberwine and co-workers,[164] direct hybridization relies on whole genome amplification of RNA. DASL uses probe sequences approximately 50 bases long and is performed by an extension−ligation reaction of two target specific sequences that bind to either side of a gene. One of these target-specific sequences also contains an encoding segment, which can bind to specific beads on the array, enabling the expressed gene to be identified. DASL can study over 500 genes at a time, and since it uses relatively short probe sequences and only 100 ng of total RNA, it is ideal for partially degraded formalin-fixed, paraffin-embedded samples. Whole-genome SNP genotyping has been performed by three techniques: (i) an allele-specific extension−ligation reaction analogous to DASL, called GoldenGate, (ii) an enzyme-based assay named Infinium I, which uses an allele-specific primer extension, and (iii) the enzyme-based Infinium II that uses single-base extension reactions. These platforms have been used to genotype over 60% of the SNP loci for the HapMap project using 'tag' SNPs in the human genome.[165] A 'tag' SNP is one that is highly correlated to nearby SNPs, thus reducing the total number of SNPs necessary for identification. These large-scale whole genome

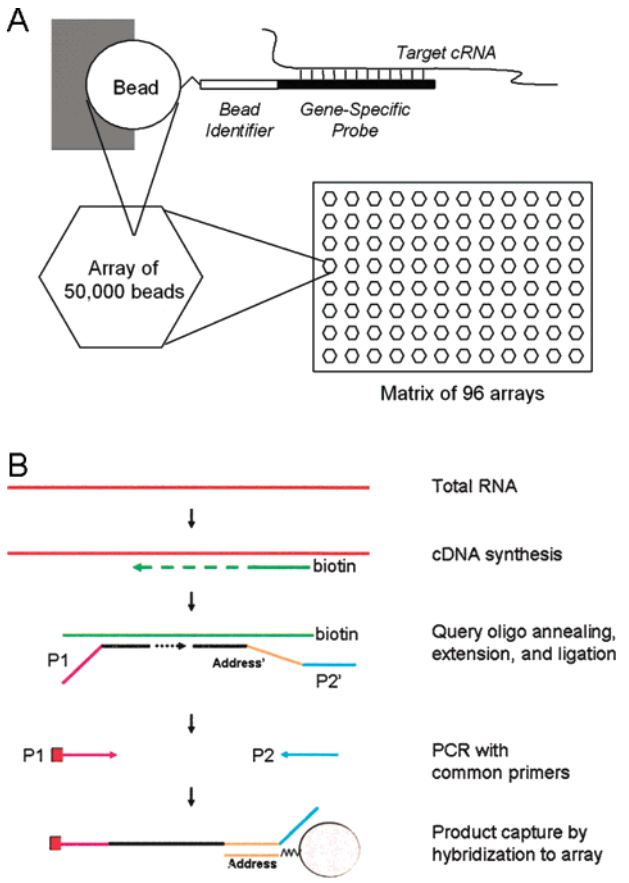

Figure 12. (A) Direct hybridization using a matrix of 96 fiber bundles. The 1.4-mm diameter optical fiber bundle contains >50 000 beads housed in wells at one end of the bundle. Each bead contains a 25-nucleotide identification sequence and a 50-nucleotide gene-specific probe. Reprinted with permission from ref 162. Copyright 2004 Cold Springs Harbor Laboratory Press. (B) Schematic of DASL, a cDNA-based assay for RNA profiling. Using biotinylated oligo-d(T)$_{18}$ and random hexamers, RNA is converted to cDNA and immobilized to a streptavidin-coated solid support. Two oligonucleotides are designed to query each target site of the cDNA. The upstream oligonucleotide consists of a gene-specific sequence and a universal PCR primer (P1). The downstream oligonucleotide consists of a gene-specific sequence, address sequences, and a universal PCR primer (P2). The upstream oligonucleotide hybridizes to the target and extends and ligates to the corresponding downstream oligonucleotide creating a PCR template that can be amplified using P1 and P2. The PCR products are fluorescently labeled and detected, using their address sequence, on beads in an array. Reprinted with permission from ref 163. Copyright 2004 Cold Springs Harbor Laboratory Press.

association studies, which cost about $0.001 per SNP,[166] have the potential to revolutionize the identification of disease-associated loci, proteins, and pharmacogenomic responses.

3.2.2.3. Protein Detection. Randomly ordered microarrays have also been used for the detection of proteins by several methods. One of the first approaches tried in our laboratory used aptamer-coated microspheres in a competitive binding study to detect the coagulation protein thrombin.[167] Aptamers are short oligonucleotides or peptides designed by an evolutionary protocol to bind specific target molecules. For the thrombin study, an anti-thrombin aptamer was bound to silica microspheres and the competitive binding curve was calibrated by measuring the fluorescent response to solutions containing a standard amount of fluorescently labeled thrombin and various concentrations of unlabeled thrombin. The system could detect 1 nM unlabeled thrombin in about 15 min. In a different experiment, the interaction of proteins and carbohydrates was probed in a multiplexed array.[168] The beads were coated with one of five synthetic carbohydrates and exposed to the fluorescently labeled protein cyanovirin N (CVN). The affinity of CVN for three of the carbohydrates was in agreement with previously reported microcalorimetry studies.

Immunoassays have been duplexed using bead-based arrays. Szurdoki et al. reported detection of the clinically important drugs digoxin and theophylline using a competitive binding assay.[169] Catalyzed reporter deposition (CARD) based on horseradish peroxidase (HRP) was used to enzymatically amplify the signal. Digoxin, in the range of 0.1−0.4 ppb, and theophylline, between 0.3 and 1.0 ppm, were detected simultaneously. Sandwich immunoassays have also been duplexed using a microsphere array for the measurement of immunoglobulin A (IgA) and lactoferrin, two immune system proteins found in saliva.[170] Mouse monoclonal capture antibodies for IgA and lactoferrin were immobilized on beads and placed in the etched wells of fiber bundle. Samples containing IgA and lactoferrin were then incubated on the sensing array for 60 min and detected using another pair of IgA and lactoferrin antibodies that were fluorescently labeled. The detection range was from 385 pM to 10 nM for lactoferrin and 700 pm to 100 nM for IgA with little cross-reactivity, suggesting multiplexed immunoassays should be possible.

The etched wells of a fiber optic bundle have also been used in a different format to determine the concentration of extremely dilute solutions of enzymes. For these measurements, the wells are used as a very dense array of microscopic reaction chambers. If the ratio of enzyme molecules to the number of wells is reduced, the Gaussian distribution describing the number of molecules per well reduces to the Poisson distribution. In this regime, the concentrations can be controlled so that only 1 or 0 enzymes will be in a well (Figure 13). Thus, a digital readout of the concentration can be made by comparing the number of wells containing one enzyme to those with zero enzymes.

Two strategies were used to confine single enzymes within the wells for low-concentration measurements. In both strategies, single molecules of the enzyme β-galactosidase were observed by observing catalysis of the substrate resorufin-β-D -galactopyranoside (RDG), which yields the yellow fluorescent compound, resorufin, after enzymatic hydrolysis. One method used a mixture of enzyme and substrate confined into single wells by pressing the fiber into an elastomeric gasket. This strategy was able to measure the concentration of β-galactosidase down to 72 fM.[171] Another method used biotinylated wells to capture streptavidin-modified β-galactosidase. The captured enzymes were then exposed to substrate using a similar gasket seal. This system was able to detect concentrations as low as 17 fM after an enzyme incubation time of 1 h.[172]

3.2.2.4. Cell Sensing. Cell-based biosensors offer an advantage over traditional receptor-based biosensors in that they measure function as well as binding. For example, chemical and biochemical sensors operate on the basis of molecular recognition and give a signal when the molecular receptor is occupied. Cell-based biosensors, on the other hand, report on bioavailability, access to target receptors, and binding. For example, a toxin must be able to traverse the cell membrane, maneuver its way to its cellular target, bind the receptor, and cause its biochemical downstream

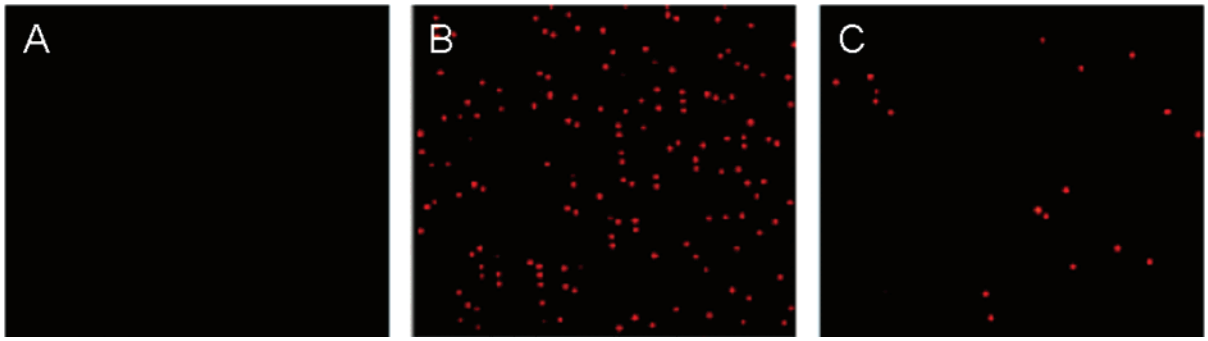

Figure 13. Monitoring the activity of β-galactosidase. (A) Background image of a portion of the fiber. (B) Portion of the fiber with a 1:5 enzyme to well ratio. (C) Portion of the fiber with a 1:80 enzyme to well ratio. (Pseudocolor added using IPlab software). Reprinted with permission from ref 171. Copyright 2006 American Chemical Society.

effect such as secondary messenger generation, gene transcription, proteolysis, etc. Furthermore, the chemical form of the analyte must be one that elicits a cellular response. For example, heavy metals can exist in numerous oxidation states and be associated with a multiplicity of ligands that can affect their bioavailability. By simply measuring metal binding to a receptor, one may be misled about the true toxicity of a sample. Consequently, cell-based biosensors provide additional information that cannot be gleaned from a simple binding event.

Cell-based biosensors in an array format offer an additional advantage over traditional high-throughput methods. Typically cellular assays, widely used in drug screening, are performed in 96-, 384-, or 1536-well plates and measure an overall response from wells containing thousands of cells. These cells, each a highly complex system, are slightly different from one another, and their physiological and genetic variabilities are masked in their collective response. In a cellular array, where each cell can be monitored continuously, the detailed stochastic nature of individual cells is revealed. Other methods to measure individual cells, such as flow cytometry,[173] can also reveal stochastic variation between cells but lack the ability to track cells over time. Only an array platform enables the monitoring of multiple cells before, during, and after exposure to various stimuli.

Arrays of single cells most often confine cells to wells, which are made by photolithography[174] or etching fiber optic bundles.[175] Soft lithography has also been widely applied to create lower density arrays of cells using either wells or patterned surface chemistries to maintain the position of a cell.[176−180] Cells have also been pneumatically trapped using an array of small orifices etched through the surface of a SOI wafer.[181] For well-based arrays, the cells are randomly assembled by sedimentation and sustained by a reservoir of nutrients held above them. Mammalian cells can maintain viability for 24 h or more,[175] and bacterial cells have been shown to be viable for more than 14 days when arrayed.[182]

While many studies involve a homogeneous cell array, analyses of mixed populations of cells have also been demonstrated. The different cells have been identified by three labeling strategies: (i) lipophilic dyes,[175] (ii) fluorescently labeled lectin,[183] and (iii) genetic encoding.[182,184] Lipophilic dye molecules are composed of a fluorophore and a long hydrophobic chain and embed themselves into the lipid bilayer of the cytoplasmic membrane. Three lipophilic dyes, PKH 26, PKH 67, and DiIC18, have been used to label mouse fibroblast cells.[175] Five fluorescent dye conjugates have also been used for labeling using the lectin concanavalin A (con A). These lectins bind to mannoproteins present on

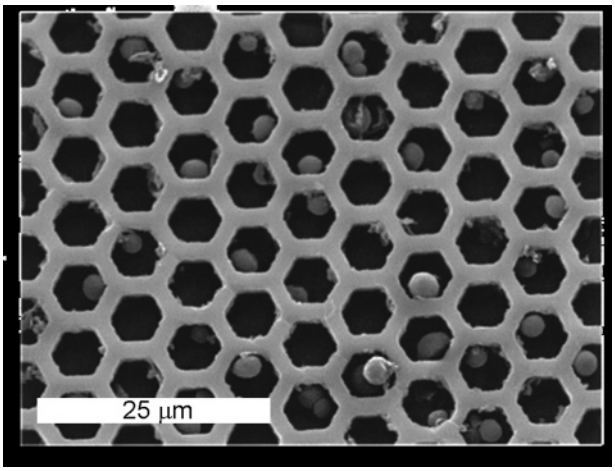

Figure 14. Scanning electron micrograph of single *S. cerevisiae* cells distributed in the wells of an etched fiber bundle. Adapted with permission from ref 183. Copyright 2002 American Chemical Society.

cell walls and were used to label five different strains of yeast.[183] The third approach, genetic encoding, uses genetically engineered cells to express fluorescent proteins, such as green fluorescent protein (GFP). This method has the advantage that it is a built-in indicator of transcription and translation and can therefore elucidate gene expression profiles while helping to distinguish different cell types contained in a multiplexed array.[182,184]

Cell noise, or the variation with which identical cells respond to their environment, has been studied in two systems, *S. cerevisiae* and *E. coli*, on an array platform.[183,184] Dye-conjugated lectins were used to label three strains of yeast to test in vivo protein−protein interactions in the yeast two hybrid (Y2H) system.[183] Yeast cells were engineered to transcribe the reporter gene *lacZ* upon protein interaction. The three yeast strains, positive (interacting proteins), negative (noninteracting proteins), and wild type, were randomly assembled into the wells of a fiber bundle (Figure 14). After decoding the array and adding a fluorogenic substrate, highly stochastic responses were obtained for the positive control strain. Further studies of this system confirm that a range of responses from ostensibly identical cells.[185] Cell noise in bacteria was analyzed by arraying two strains of *E. coli* carrying the fusions *recA::gfp* and *lacZ::gfp*.[184] For both *recA* and *lacZ* the expression became noisier with time. In the induced state, *lacZ* showed 5 times greater noise compared to *recA*, possibly due to its more complex gene network. The information-rich data of these studies, showing the stochastic nature of gene translation and transcription

dynamics, could only be collected from cellular arrays.

Cellular arrays have also been used for toxicity and drug screenings and identify and isolate antigen-specific B-cells. Genetically engineered *E. coli* was used to measure as low as 100 nM Hg^{2+}, based on the expression of reporter genes.[186] In another study, the effectiveness of the antimigratory drug nocodazole was verified by monitoring rates with which individual cells traversed the optical cores of a fiber optic bundle.[187] A third report used a very high density array ($>140\,000$ wells/cm^2) of single lymphocytes to identify antigen-specific B-cells.[188] The response from each cell was measured after exposure to an antigen, and responsive cells were isolated from the array by a micromanipulation pipet. These three studies exemplify the benefit of functional biosensors—because cells are alive, they can measure things beyond just binding. Cell-based sensors also measure bioavailabilty, access to key cellular components, and show the effect on the overall biological system.

Despite the aforementioned benefits of cellular arrays, there are several issues that have limited their commercialization.[189] One issue is well size—since cells come in many shapes and sizes, there is no universal well size that works for all cell types. An assortment of well sizes would likely be necessary for different experiments. Likewise, for bacteria and yeast cells, wells should be only a few micrometers in diameter. This size is somewhat challenging because it coincides with the smallest feature sizes achievable on a typical mask aligner used for photolithography. Another concern is the ability of cells to communicate with each other when confined to wells. Work needs to be performed to prove that collections of separated cells respond in the same way as a collection of unconstrained cells. Finally, it is extremely difficult to isolate individual cells from the array for further analysis, such as gene expression. Technical improvements in array manufacturing and cell manipulation, as well as further studies into the biological consequences of isolating cells, will likely lower the barriers of commercializing cellular arrays.

3.2.3. Cross-Reactive Sensing Arrays

A sensing element that has a broad range of specificity and responds to a wide variety of analyte species is known as a cross-reactive sensor. Evaluation of an analyte by a cross-reactive array is based on the overall response pattern of the array for the unknown substance in comparison to the response pattern from known controls.[190] The scheme is based loosely on principles of the mammalian olfactory system. In some mammalian olfaction systems, millions of olfactory receptor neurons respond to a given odor with each neuron expressing only one type of receptor out of a repertoire of ca. 1000 receptors. The various responses of these neurons are sent to the brain for processing where the pattern is recognized based on previous exposure to similar mixtures, thereby creating an odor memory. Every receptor (and neuron) responds to many different vapors but differentially such that with 1000 different receptors a nearly infinite number of patterns can be generated.

This combinatorial advantage enables sensor arrays to be created that do not rely on traditional "lock and key" binding. Specificity is encoded in the response pattern rather than in any specific sensor; hence, the term "distributed specificity" has been applied to this approach.[191,192] An "artificial nose" based on the principles of cross-reactivity employs many semi-selective sensing elements. In this approach, a pattern recognition algorithm must be trained first to recognize the vapors of interest. When the sensor array is subsequently exposed to a vapor in the database, the algorithm compares the response of an unknown vapor to the responses from prior training. This technology could have broad applications ranging from monitoring food and air quality to detecting explosives.[193]

Sensors with broad response use physical and chemical properties common to all molecules such as polarity or hydrophobicity. Analyte molecules can span the continuum of a given physicochemical property. Using a single sensor is insufficient to detect very similar analytes because their physicochemical properties may be similar. Multiple sensors, responsive to different properties or in different ranges, must be used to distinguish between molecules with similar properties. Transduction mechanisms for a variety of physicochemical properties have been demonstrated to create cross-reactive sensors. One transduction mechanism is the adsorption of gas in metals,[194] metal oxides,[195] semiconductors,[196] or conducting polymers,[197] which changes their conductive properties, enabling electrical measurements of vapor samples. Solvatochromic dyes,[152] ion-selective electrodes,[198] and surface acoustic wave sensors[199] have also been used in cross-reactive detection.

In very high density fiber optic bead arrays, solvatochromic dyes such as Nile Red are adsorbed onto the surface or entrapped in various polymer or porous silica beads.[152] When a vapor is sorbed into the polymer beads, the fluorescent reporter shifts wavelengths and/or intensity based on polarity changes in the bead during exposure to analyte vapors. The different bead types have different polarities and consequently exhibit different spectral and sorption properties. A time trace of these changes is collected from all the beads in the array using the optical system with image acquisition software. Other factors also influence the time trace, such as the porosity of the bead, its ability to swell, and its hydrophobicity. By using a system like the one shown in Figure 9 to monitor fluorescence traces versus time over different bead types, characteristic responses profiles are generated for different analytes. The response pattern of known analytes, depicted in Figure 15, can then be used to train pattern recognition software, such as artificial neural networks, in order to classify the response of unknowns.[200]

As discussed above, the different bead types in this array are distributed randomly. Because like elements of the array respond the same, they can be readily identified by exposing them to a known test vapor because the response pattern from a given sensor type to a given vapor is reproducible. This 'self-encoding' mechanism allows the random array to be decoded if desired. A separate decoding step is not necessary, however, because cross-reactive arrays make an identification using response patterns and, as long as the sensors and responses are reproducible, can be compared to a response library.[201]

There are many advantages to having a very high density cross-reactive sensor array. One benefit is analogous to the NEEs where small individual signals measured by each element of the ensemble are integrated to give a large collective response. Since there can be many thousands of beads with the same sensing dye, their responses can be combined to amplify what may be a very small fluorescence signal or signal change.[152] Another advantage is the increased sensitivity and rapid response time, typically a few seconds, of the microspheres due to their small size and high surface to volume ratio. The microsphere platform also improves

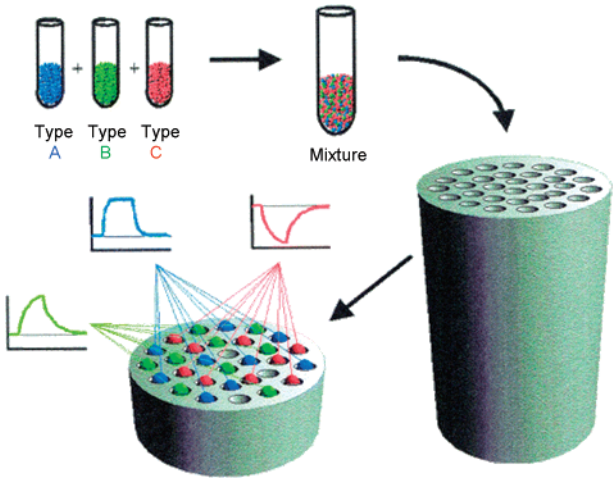

Figure 15. Schematic illustration of a self-encoded bead array. A mixture of sensor beads is prepared by combining beads from three stock solutions. A drop of the mixture is placed on the etched end of a fiber optic bundle. The beads are identified and categorized by the characteristic responses to a test vapor pulse. Since the analytical signal of each bead also identifies the bead and maps its position in the array, the beads are self-encoding. Reprinted with permission from ref 152. Copyright 1999 American Chemical Society.

array to array reproducibility because millions of identical beads are created and stored together. This reproducibility allows a training database to be carried over from array to array despite the differences in location of the beads between two arrays.[202] By summing all identical bead types in an array, slight bead-to-bead variations are also eliminated. While these features make this system attractive, it still suffers from some drawbacks. One problem is sensor poisoning upon exposure to reactive analytes. Another drawback is photobleaching of the dye over long periods of time. Strategies such as illuminating subsections of the array and using an adaptive light exposure scheme by beginning the experiment at low illumination levels and gradually increasing to compensate for photobleaching have been developed to avoid this problem.[203]

Fiber optic cross-reactive sensing arrays have been demonstrated in artificial nose applications to detect nitroaromatic explosive-like compounds (NACs) and complex vapor mixtures such as distinguishing brands of coffee and living/dead bacteria. NACs like 1,3-dinitrobenzene (DNB) and 2,6-dinitrotoluene have been detected at ppb levels, even in the presence of volatile organic compounds, such as toluene and benzene, at levels thousands of times higher.[204] The sensors were shown to have a shelf life of at least 10 months, and their responses were highly reproducible. The complex odor samples consisted of three varieties of coffee bean along with acetone, toluene, and DNB.[205] Using discriminant functional analysis, these six samples could be identified with 100% accuracy at high concentration levels and 85% accuracy at lower levels. Larger numbers of vapors have also been classified. More specifically, 20 odor compounds consisting of several alcohols, alkanes, aromatics, and several two-component mixtures were distinguishable with greater than 90% accuracy using between 6 and 18 sensor types (Table 2).[201] The ability to 'learn' the profile of a large number of vapors and distinguish chemically similar species rapidly, in high backgrounds, is necessary to realize the goal of real-time vapor detection systems for applications ranging from monitoring food quality to national security.

Table 2. Odor Discrimination Accuracy for 100 Odor Exposures When All Sensor Responses Are Combined (Nondecoded Arrays)[a]

	classification rate (%)	
array type	trial I	trial II
single sensor	74	74
single sensor	86	98
single sensor	76	94
03-bead random	80	98
06-bead random	86	97
09-bead random	93	94
12-bead random	95	94
15-bead random	85	98
18-bead random	97	96

[a] Three distinct response patterns are obtained for fluorescence vs time traces for three different beads types after exposure to the same vapor. All arrays in trials I and II employed different microsensor types, even for the 01-bead arrays. The only arrays with the same sensor composition for I and II were the 18-bead arrays (see ref 201). Twenty different odor exposures (5 replicates each): (1) air carrier gas, (2) acetone, (3) *n*-heptane, (4) ethanol, (5) toluene, (6) water, (7) ethanol/heptane mixture 1:1 (v/v), (8) methanol/ethanol mixture 1:1 (v/v), (9) benzene, (10) 1-propanol, (11) aqueous 90 ppb 1,3-dinitrobenzene, (12) 1,3-dinitrobenzene (s), (13) methanol/1-propanol mixture 1:2 (v/v), (14) methanol, (15) 1-butanol, (16) 3-pentanol, (17) *p*-xylene, (18) ethanol/1-pentanol mixture 1:3 (v/v), (19) cyclohexanone, and (20) 1-pentanol. Since there were 100 observations, the number of misclassifications is apparent from the classification rate ((97%) 3 mistakes; (86%) 14 mistakes). Reprinted with permission from ref 201. Copyright 2003 American Chemical Society.

3.3. Suspension Arrays

3.3.1. Introduction

A third class of very high density arrays is suspension arrays. Unlike the previously mentioned arrays, suspension arrays are not in a fixed 2-D pattern. Instead, the array elements, which typically consist of microspheres, are free floating or suspended in solution. While the term "array" is probably a misnomer, this terminology is used to describe assays performed on microparticles in solution. This type of array is considered very high density because the typical element size is about 5 μm in diameter. Because the elements are not in a fixed pattern, it is impossible to analyze the array with the same detection methods that are used for planar arrays, such as imaging. Instead, the microparticles are scanned individually. The methods used for scanning microparticles in solution have their roots in flow cytometry.

Flow cytometry is a well-established method of counting, sorting, and examining microparticles. Initially developed in the 1970s for cell counting and sorting, flow cytometry works by hydrodynamically focusing particles from a sample into a narrow stream where the particles move in single file.[206] The particles pass through the beam of a laser, and the scattered light and/or any resulting fluorescence is detected (Figure 16). Particles can be scanned at rates up to 100 000 particles per second, and several lasers or detectors can be used simultaneously for multiparameter analysis.

For multiplexed suspension array assays, standard cytometry equipment can be used, but the microcarriers must be encoded to identify which analyte they are sensing. Several reviews have been written on the topic of suspension arrays[207−209] and their encoding,[210,211] but in general there are two main encoding options—spectral or graphical. The more established encoding method is spectral and usually done by fluorescent labeling. Dye labeling with multiple

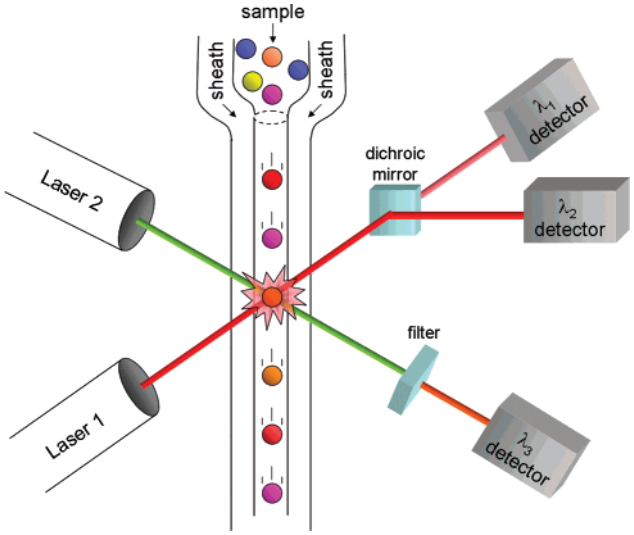

Figure 16. Schematic illustration of a flow cytometer used in a suspension array. The sample microspheres are hydrodynamically focused by a sheath fluid and passed through two laser beams. The fluorescence caused by laser 1 is detected at two wavelengths to identify the encoding dyes to determine which analyte the microsphere captures. Laser 2 excites fluorescence at a third wavelength and is used to quantify the bound analyte.

fluorophores in several concentrations has been commercialized for the encoding of up to 100 bead types by Luminex Corp. (Austin, TX). Luminex uses orange and red fluorescent dyes for encoding and a third dye, often green, for analysis. The 5.6 μm polystyrene beads can be identified and measured at a rate of about 1000 per second. With this throughput, a 100-plex assay consisting of ~200 duplicates of each bead type could be read in about 30 s. This acquisition rate would enable nearly 3000 100-plex assays to be performed per day.[209] While these numbers are impressive, the maximum number of about 100 encoding combinations is limited compared to the multiplexing available in planar arrays.

The other encoding method, graphical encoding, promises a much higher degree of multiplexing. Graphical encoding is done by imprinting an identifying code into a particle based on its size, shape, or composition (Figure 17). For example, silica nanowires that are composed of thick and thin segments of various sizes can be visibly distinguished from one another.[212,213] Likewise, nanowires made of silver and gold layers can be identified by the pattern length and frequency of the different metal segments.[42] More elaborate graphical encoding schemes have recently been examined by Doyle and co-workers.[214] By combining photolithography and microfluidics, Doyle created microcarriers that resemble computer punch cards. These pill-shaped microparticles are on the order of 100 μm in width and 300 μm in length; the encoding region occupies about one-half of the microparticle area with the remaining portion being used for analysis. This scheme has the potential to produce millions of encoding combinations for highly multiplexed detection but has thus far only been demonstrated on a small scale with several analytes. While still in its infancy, graphical encoding seems very promising and will likely be the focus of many future applications.

The established microsphere-based technology has been used by many groups for various multiplexed analysis with several thousand Luminex systems in place for both research and clinical applications.[215] Protein detection has been performed for a wide range of applications. As will be described, suspension arrays have also been used for nucleic acid analysis, such as genotyping and gene expression.

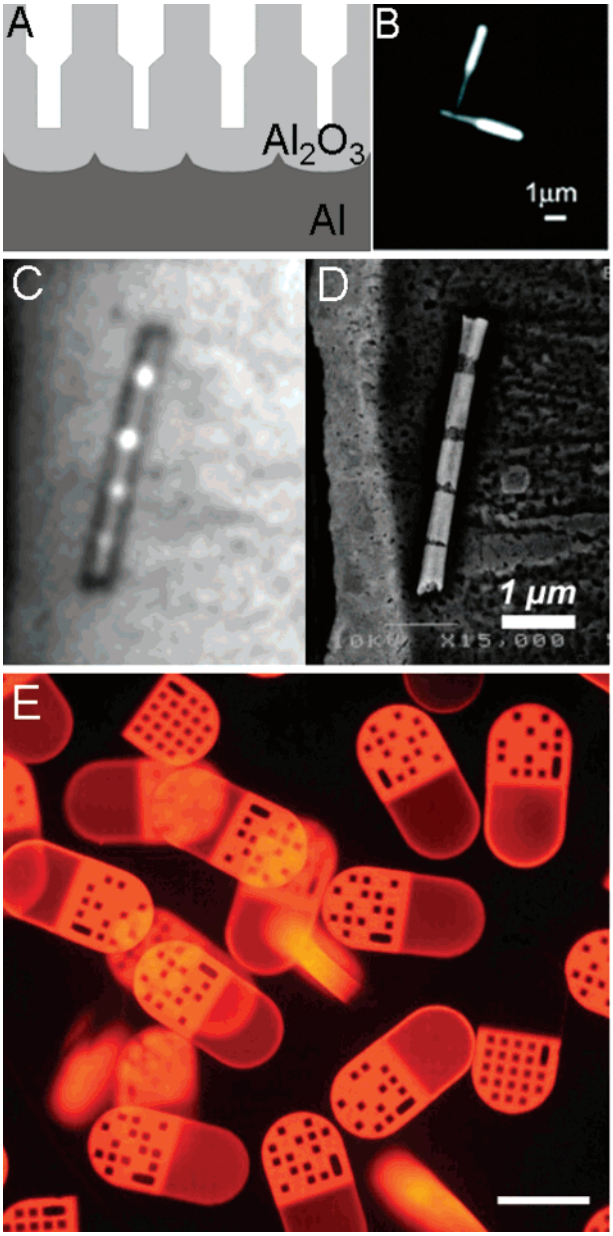

Figure 17. (A) Schematic of an alumina template used to create shape-encoded silica nanotubes. Adapted with permission from ref 212. Copyright 2006 American Chemical Society. (B) Dark-field optical micrograph of silica nanotubes prepared using template shown in A; the larger diameter segments are more reflective and therefore look brighter. Reprinted with permission from ref 213. Copyright 2006 American Chemical Society. (C) Optical and (D) FE-SEM micrographs of a single Au−Ag multistriped particle. The gold sections are ~550 nm in length, and the silver sections range from 60 to 240 nm in length. Reprinted with permission from ref 42. Copyright 2001 American Association for the Advancement of Science. (E) Optical micrograph of dot-coded polymer microparticles. One-half of the particle is for encoding, while the other half is used for analyte detection. Scale bar = 100 μm. Reprinted with permission from ref 214. Copyright 2007 American Association for the Advancement of Science.

3.3.2. Protein Detection

The use of suspension arrays for protein detection was proposed as early as 1977 and has been used extensively for immunoassays for over 20 years.[206,216−218] Fulton et al.

completed pioneering work in the area of multiplexed immunoassays by testing canine serum for IgG and IgE antibodies specific to 16 grass allergens simultaneously.[219] Similarly, Carson and Vignal detected 15 cytokines, including IL-2, IL-4, and IFN-γ, using only 100 μL of sample.[220] Using a more traditional enzyme-linked immunosorbent assay (ELISA) would require 100 μL for each of the 15 cytokines in the assay. Other studies confirmed that suspension arrays are more reproducible, have a greater dynamic range, and require less preparation time than conventional ELISA.[221]

Immunoassays performed on suspension arrays have been used to measure allergens, toxins, and even explosives. The binding affinity of 17 plant lectins, such as peanut and wheat germ agglutinin, for 13 different glycoproteins was measured on a suspension array.[222] Microspheres were prepared by coating their surface with one of the 13 glycoproteins, and then the 13 bead types were exposed to biotinylated lectins. After incubation, the lectins were labeled using R-phycoerythrin-conjugated streptavidin, and the binding was measured through flow cytometry. The determined affinities were in good agreement with previously reported values.[222] In another study, a library of single-domain antibodies (SdAb) from llamas was created and screened using a suspension array to find SdAbs that bound toxins, such as ricin and cholera.[223] The antigen binding arms, or V domains, of SdAbs are particularly interesting; because they are the smallest natural binding domains, they are inherently thermostable and because they can often refold after denaturation. Error-prone PCR SdAb genes from three llamas were mutated to create SdAbs that would selectively bind one of six toxins.[223] In another screening study, six antibodies were designed to bind TNT and other nitroaromatics and tested in a competitive binding study. The best antibody could detect between 0.1 ppb to 10 ppm of TNT.[224]

Suspension array-based immunoassays have also been used for exploring the detection and mechanisms of viruses, such as influenza and HIV. For example, the influence of HIV on plasmacytoid dendritic cells (pDCs) has been studied using a suspension array system made by BD biosciences (San Jose, CA).[225] It was shown that HIV-1 g120 interferes with pDCs ability to secrete type I IFNs. Similarly, experiments using an unusually severe influenza virus from 1918 were completed on non-human primates. Results from a suspension array-based immunoassay revealed that this strain has the ability to modulate the innate immune response of the host, which could be a common trait among virulent influenza viruses like avian H5N1.[226]

3.3.3. Nucleic Acid Detection

In 2001, Yang et al. described the use of a suspension array for gene expression.[227] Using fluorescently encoded microspheres, they were able to quantify the presence of 20 RNA sequences in each sample. Sample RNA was amplified by PCR with biotinylated primers and then captured by cRNA immobilized on microspheres. Following streptavidin−phycoerythrin labeling, the beads were analyzed on a flow cytometer. One advantage of this method is that large numbers of different cRNA beads are made and can be aliquoted for use in many experiments. This method fills a niche not served by other methods of gene expression, such as high density lithography arrays, because it is a fast and cost-effective way to test a relatively small number of genes in a large number of samples.

More recently, gene expression has been performed using suspension arrays to compare the expression of micro RNAs (miRNAs) between cancerous and healthy cells.[228] Suspension arrays were chosen for this study because the short size of miRNAs (~21 nucleotides), and the similarity between miRNA family members often causes cross-hybridization on planar glass slide arrays. A study was performed comparing the extent of cross-hybridization to each of the two different array formats, and the suspension arrays performed better than the planar arrays for all 11 miRNAs tested. Overall, results from the analysis of 217 mammalian miRNAs from 334 samples found a general trend toward down regulation of miRNAs in tumor cells compared to healthy cells. The researchers also observed that poorly differentiated tumors could be classified by miRNA analysis more effectively than by mRNA profiling.

Suspension arrays have also been used to multiplex the detection of mRNA using a sandwich assay with amplification technology involving branched DNA (bDNA).[229] In this method, capture probes on microspheres bind to multiple locations on the target mRNA. Highly branched DNA labeled with biotin can then bind to the mRNA to form the sandwich. A streptavidin−phycoerythrin conjugate is then used to tag the bDNA, indicating the presence of the mRNA. This technique does not amplify or purify the target mRNA and can be used to analyze crude cell lysates or tissue homogenates. Flagella et al. multiplexed their assay to simultaneously detect 10 mRNA sequences with sensitivity down to 25 000 RNA transcripts.[229]

Several methods of SNP genotyping have also been demonstrated using suspension arrays. A direct hybridization technique was used by coating four types of fluorescently encoded microspheres with four oligonucleotides that varied by only a single base.[230] The labeled target then bound to only one of the four bead types identifying the SNP; eight SNPs have been detected in this way, requiring 32 bead types. Two other methods, known as oligonucleotide ligation assays (OLA)[231] and single base chain extension (SBCE) assays,[232,233] have also been used. Highly analogous to the GoldenGate and Infinium assays developed by Illumina Inc., OLA and SBCE use microspheres coated with oligonucleotides that act as address encoders, known as ZipCodes, for binding amplified and labeled product. Unlike the Illumina encoding method, however, ZipCodes are not sufficient to identify the microsphere; instead, the microspheres are still fluorescently encoded, and the ZipCode acts as an intermediate linker to associate a particular bead with a particular SNP call. These methods have been used to identify over 50 SNPs simultaneously.[232] While fluorescently encoded suspension arrays are far below their planar array counterparts in terms of the number of SNPs they can call, they may fill a niche where a small number of SNPs need to be rapidly genotyped among a large number of samples.

4. Future Directions

There are many promising materials and technologies that one day may enable the preparation of very high density sensing arrays. In some cases, substrates have been created with feature sizes suitable for implementation with very high density sensing arrays. In other cases, functional materials containing both array characteristics and the ability to transduce signals exist. Other technologies exist that may one day enable the readout of very high density sensing arrays at scales that cannot be achieved using today's technologies.

4.1. Substrates and Materials

4.1.1. New Materials

Materials scientists are developing a significant number of new substrates that offer potential platforms for very high density sensing arrays. One of the most promising of these substrates is anodically etched alumina, which has been used for the NEEs. Martin and co-workers recently used the alumina nanopore membrane as a mask by overlaying it on a polymer during a plasma etching process. After removing the alumina mask, a regular array of nanopores is created.[31] Silica can be deposited in these nanopores to produce nano test tubes.[43] The diameter of these test tubes is approximately 85 nm, and the depth can be controlled by the length of plasma etching. These alumina membranes can also be etched to produce an array of conical nanopores, which have been used as synthetic resistive-pulse sensors for stochastic measurement of biomedical analytes.[234] As the fabrication of these conical pores becomes more reproducible, use of artificial-nanopore biosensors will likely become more widespread.[235]

A wide variety of other promising materials exist with the potential for creating very high density sensing arrays. Such materials include wire ensembles (e.g., carbon nanotubes, metal wires),[236−238] colloidal crystal arrays,[239,240] self-assembled nanostructures,[241,242] polymeric and silica microsphere monolayers,[57] and metal nanoparticle arrays.[243] All of these materials offer attractive and tantalizing substrates for creating a variety of different very high density array architectures. The ability to capitalize on these materials will depend on the ingenuity of materials scientists, chemists, and life scientists.

4.1.2. Functional Materials

At a higher level of sophistication are functional materials in which, in addition to an array format substrate, some form of function is integrated. For example, zinc oxide nanowire ensembles have been created.[244] ZnO nanowires have been grown epitaxially on an alumina substrate using gold particles as a catalyst. The resulting nanowires exhibit a piezoelectric effect such that mechanical stimulation of the wires leads to an electrical signal. This approach integrates both array fabrication with a transduction mechanism. At present, this approach remains relegated to an ensemble as all the nanowires are connected to a single readout device.

Another approach to functional sensors employs molecular valves. In this approach, rotaxanes are attached at the openings of mesoporous silica nanopores.[245−247] The rotaxanes can be switched to one of two conformations using an electrochemical or redox reaction resulting in opened or closed nanopores. Consequently, the rotaxanes act as nanovalves to open or close a channel. While exhibiting a functional response, all nanovalves are comprised of the same rotaxanes resulting in a uniform response of the entire material. In addition, the valves do not exhibit selectivity in the types of molecules that are released or allowed to enter from the pores. By integrating chemical selectivity into such nanovalve arrays, it may be possible to create extremely high density sensor arrays.

Recently Aizenberg and co-workers reported very high density ensembles of hydrogel nanocolumns that were responsive to humidity.[248] The shapes of the nanocolumns could be controlled by the stress field in the hydrogel. The regular pattern of nanoscale features combined with an intrinsic responsivity suggests that mechanical transducers with built-in response mechanisms can be fabricated. A host of hydrogel sensors already exists that are responsive to a variety of chemicals such as ions, glucose, and neurotransmitters that could be integrated into such arrays.[72−74]

In this context, the ability to create new materials or readout mechanisms that do not require labels is one of the major future goals for any sensing method. By using the intrinsic signals of the materials upon binding analytes or developing new readout methods that can detect analyte binding, it should be possible to simplify array design and increase the level of multiplexing significantly.

4.2. Novel Array Designs

4.2.1. Molecular Arrays

Perhaps the ultimate in density will be when single molecules can serve as the array elements. For example, Bayley and co-workers have been developing elegant methods for engineering α-hemolysin—a pore protein that in its natural form punctures red blood cell membranes.[249] The engineered forms of α-hemolysin can be designed with molecular specificity to allow specific molecules to traverse the pores. By measuring the conductivity of the membranes, stochastic binding events can be measured from single analyte molecules binding to the pore.[249] If these pores can be arranged in an array format and measured individually, they will offer an unprecedented density of molecular sensors.[234]

Seeman and co-workers recently reported their ability to tile DNA structures with pendant arms that enable molecular attachment and recognition.[250,251] This approach offers a spectacular demonstration of self-assembly and offers the potential for creating molecular arrays with the ability to direct multiple and different receptors to defined sites.

4.2.2. Liquid Arrays

A revolutionary approach to creating very high density sensing arrays involves creation of liquid or "virtual" arrays. In this approach, optical traps are employed to capture microspheres or cells in liquids. Optical traps, also called optical tweezers, are created by focusing a high-intensity laser to a small spot. Because of the refractive index differences between particles and the liquids in which they reside, momentum can be imparted to the particle such that the particle is confined to the focal point of laser beam. Recently, arrays of optical traps have been created using holography[252] or optical fibers.[253] By integrating microfluidics with these systems, it is possible to trap many particles simultaneously in either two or even three dimensions. Individual traps can be controlled to either hold or release a given particle or cell. One can imagine using such microsphere arrays to analyze samples, release the microspheres when they are exhausted, and then create another array out of fresh microspheres without the need for any substrate.

4.3. New Tools and Devices

4.3.1. Optical

One of the existing limitations for very high density sensing arrays is the ability to read out the individual sensing elements at the requisite resolution. A number of optical methods for breaking the diffraction limit of light have been developed recently and offer the potential to be used for array

readout. One of the earliest methods for breaking the diffraction limit is near-field scanning microscopy (NSOM). This method is still relegated to the laboratory and a relatively slow technique.

More rapid techniques using more conventional microscope platforms have been developed recently. For example, the stimulated emission depletion (STED) approach involves illuminating a sample with a highly focused laser beam to excite a fluorescent dye while simultaneously illuminating with a doughnut-shaped beam to deexcite fluorophors outside the region of interest.[254,255] Using STED microscopy, resolutions of 20 nm can be achieved, potentially enabling the ability to read extremely high-density arrays or ensembles. Another method is the sub-diffraction-limit imaging by stochastic optical reconstruction microscopy (STORM).[256,257] In this approach, only a fraction of the fluorophors in an image field is excited. By building up a series of fluorescence images, each with sub diffraction resolution of multiple sites within the field, it is possible to achieve resolutions of 20 nm.

4.3.2. Surface Readout

STM, AFM, and related methods have been the cornerstone of surface analysis over the past decade. With the ability to scan more rapidly using less expensive and smaller systems, the ability to integrate surface readouts with very high density sensing arrays in an inexpensive format is on the horizon. The work of Mirkin and co-workers in preparing a very high density of cantilevers for dip-pen nanolithography should make such readout devices practical.[90]

There has been a revolution in device fabrication over the last several decades. For example, CCD chips are now commonplace in digital cameras; CMOS devices are in children's toys; microfluidics and MEMS systems are pervasive. These devices will undoubtedly enable a transformation of the very high density array field over the next few years. CMOS devices are of particular note as they are inexpensive and possess on-chip processing. They are megapixel devices with all the integrated circuitry. One can imagine that these devices may be used directly for fabricating sensor arrays by simply attaching different chemistries at different pixel locations.

4.4. Novel Applications of Very High Density Sensing Arrays

In the most optimistic scenario very high density sensing arrays containing thousands to millions of individually addressable nanoscale elements will be accessible. Assuming that the requisite chemistries for performing molecular recognition of thousands of different species is developed, such arrays will have the capability for performing a high level of multiplexed sensing or analysis. Such arrays will have tremendous functionality, be inexpensive because the materials costs will be low (due to the small amounts of material required), and should provide a universal platform for low-cost analysis. These arrays may have specific sensors, cross-reactive sensors as discussed above, or both.

Advances in cell-based sensing arrays could revolutionize functional sensing (vide supra) by enabling rapid and high-content screening for new drug candidates including absorption, distribution, metabolism, excretion, and toxicity.[258] The ability to array different types of cells in precise locations also offers the possibility to design tissue mimics and understand how different cell types communicate and affect one another.

Langer and co-workers developed a controlled release drug delivery array in which reservoirs can be filled with drugs and sealed.[259] The back of the array has microcircuitry that allows the release of drugs from different regions of the chip upon electrical actuation. As the array reservoirs become smaller and methods are developed for loading different drugs in different regions of the chip, the ability to control release on a much finer scale will be possible. In addition, sensors may one day be integrated into the array to enable simultaneous analyte sensing and multidrug controlled release. Such arrays could find use as implantable monitoring devices for detecting an oncoming illness (e.g., infectious disease or heart attack) and autonomously take action by releasing drugs or nutrients to prevent their occurrence.

Other manifestations of very high density sensing arrays will enable tremendous advances in fundamental science. For example, arrays of many individual cells can be simultaneously interrogated using sensitive patch clamp techniques, which will enable functional sensing for drug discovery applications.[260] Arrays of fully functional genes that can be translated into proteins localized to the region where they are translated will enable studies of protein−protein interactions as well as biochemical pathways.[261] Maerkl and Quake recently demonstrated the ability to integrate a fluidic delivery system with a DNA microarray to measure transcription factor binding constants.[262] As arrays become higher density and multifunctional, the ability to collect fundamental chemical, biochemical, and biological information will increase.

4.4.1. Next-Generation Sequencing

One of the most exciting contemporary areas in life sciences technology is the field of next-generation sequencing. Over the last several years the cost of de novo sequencing has been reduced more than 2 orders of magnitude as a result of new technologies. In most of these technologies, a single molecule of DNA is amplified either on a bead or after binding to a surface. In the former approach, each bead represents a "clone" of a particular sequence and the library of beads is then spread onto a substrate or confined in microwells. In the latter approach, each single DNA molecule is replicated manyfold and confined to a small spot on a substrate. Using a series of biochemical steps such as elongation, ligation, dye attachment, and/or hybridization, the sequences of the immobilized DNA can be determined. Sequence determination is conducted in parallel on many thousands to millions of DNA strands simultaneously. Most of this work is being carried out by commercial entities. All of these approaches employ random arrays in which the positions of particular DNA molecules are undetermined. In some cases, the array format is identical to existing very high density sensing arrays such as the 454 sequencing technology that relies on fiber optic microwell arrays as described above.[263] In other cases, such as the Solexa[264] or Agencourt[265] approaches, single DNA molecules are amplified and deposited randomly on a planar substrate. In perhaps the highest density approach, Helicos is pursuing similar technology in which random arrays of single DNA molecules are sequenced with no amplification.[266]

4.5. Issues

One of the most significant issues with very high density sensing arrays is the lack of methods to prepare arrays

containing different features in different locations. For example, molecular receptors if configured properly can be used to create sensors. Even if very high density array substrates are available, with present day technology it is painstaking to put different receptors in different locations of an array in a precise and registered manner. Although dip-pen nanolithography offers a set of tools for accomplishing this task, it is not amenable to all array formats.

A related issue is connecting the arrays such that individual signals from each array element can be detected. With optical methods, direct connections are not necessary; however, with electrical and/or mass measurements, a direct connection to the transducer is required. Direct connections to the different array elements must also be to an external readout device. Readout devices for both optical and electrical measurements must be small and inexpensive for most very high density array applications; otherwise, the use of such arrays will be relegated to research laboratories.

Despite the issues discussed above and the challenges remaining before very high density sensing arrays achieve their full potential, the transformation has been remarkable in terms of the short time it has taken to move from single measurements to the high density high-content array formats in use today. The opportunities presented by new materials, devices, and tools, coupled with the clever designs of scientists working at the micro- and nanoscales, promises rapid advances in very high density sensing arrays that will permanently transform the fields of measurement science and life sciences.

5. Acknowledgments

We would like to acknowledge the TEACRS program of the NIH/NIGMS as well as the Howard Hughes Medical Institute for supporting this work. Assistance from members of the Walt lab, including Timothy Blicharz, Ragnhild Whitaker, Ryan Hayman, and Dr. David Rissin, is also acknowledged.

6. References

(1) Tehan, E. C.; Higbee, D. J.; Wood, T. D.; Bright, F. V. *Anal. Chem.* **2007**, *79*, 5429.
(2) Schena, M.; Heller, R. A.; Theriault, T. P.; Konrad, K.; Lachenmeier, E.; Davis, R. W. *Trends Biotechnol.* **1998**, *16*, 301.
(3) Bowtell, D. D. L. *Nat. Genet.* **1999**, *21*, 25.
(4) Schena, M. *Microarray Analysis*; John Wiley & Sons Inc.: Hoboken, NJ, 2003.
(5) Penner, R. M.; Martin, C. R. *Anal. Chem.* **1987**, *59*, 2625.
(6) AlMawlai, D.; Coombs, N.; Moskovits, M. *J. Appl. Phys.* **1991**, *70*, 4421.
(7) Wightman, R. M. *Anal. Chem.* **1981**, *53*, 1125A.
(8) Dayton, M. A.; Ewing, A. G.; Wightman, R. M. *Anal. Chem.* **1980**, *52*, 2392.
(9) Štulik, K.; Amatore, C.; Holub, K.; Marecek, V.; Kutner, W. J. *Pure Appl. Chem.* **2000**, *72*, 1483.
(10) Zoski, C. G. *Electroanalysis* **2002**, *14*, 1041.
(11) Bard, A. J.; Crayston, J. A.; Kittlesen, G. P.; Varco Shea, T.; Wrighton, M. S. *Anal. Chem.* **1986**, *58*, 2321.
(12) Hulteen, J. C.; Menon, V. P.; Martin, C. R. *J. Chem. Soc., Faraday Trans.* **1996**, *92*, 4029.
(13) Davies, T. J.; Compton, R. G. *J. Electroanal. Chem.* **2005**, *585*, 63.
(14) Saito, Y. *Rev. Polarogr.* **1968**, *15*, 177.
(15) Menon, V. P.; Martin, C. R. *Anal. Chem.* **1995**, *67*, 1920.
(16) Davies, T. J.; Ward-Jones, S.; Banks, C. E.; del Campo, J.; Mas, R.; Munoz, F. X.; Compton, R. G. *J. Electroanal. Chem.* **2005**, *585*, 51.
(17) Jeoung, E.; Galow, T. H.; Schotter, J.; Bal, M.; Ursache, A.; Tuominen, M. T.; Stafford, C. M.; Russell, T. P.; Rotello, V. M. *Langmuir* **2001**, *17*, 6396.
(18) Thurn-Albrecht, T.; Schotter, J.; Kastle, G. A.; Emley, N.; Shibauchi, T.; Krusin-Elbaum, L.; Guarini, K.; Black, C. T.; Tuominen, M. T.; Russell, T. P. *Science* **2000**, *290*, 2126.
(19) Martin, C. R. *Chem. Mater.* **1996**, *8*, 1739.
(20) Martin, C. R. *Science* **1994**, *266*, 1961.
(21) O'Sullivan, J. P.; Wood, G. C. *Proc. R. Soc. London A* **1970**, *317*, 511.
(22) Li, A.-P.; Muller, F.; Birner, A.; Nielsch, K.; Gosele, U. *Adv. Mater.* **1999**, *11*, 483.
(23) Masuda, H.; Fukuda, K. *Science* **1995**, *268*, 1466.
(24) Fleisher, R. L.; Price, P. B.; Walker, R. M. *Nuclear tracks in solids: Principles and applications*; University of California Press: Berkeley, CA, 1975.
(25) Tierney, M. J.; Martin, C. R. *J. Phys. Chem.* **1989**, *93*, 2878.
(26) Parthasarathy, R. V.; Martin, C. R. *Nature* **1994**, *369*, 298.
(27) Wilson, J. N.; Bangcuyo, C. G.; Erdogan, B.; Myrick, M. L.; Bunz, U. H. F. *Macromole.* **2003**, *36*, 1426.
(28) Lakshmi, B. B.; Patrissi, C. J.; Martin, C. R. *Chem. Mater.* **1997**, *9*, 2544.
(29) Che, G.; Jirage, K. B.; Fisher, E. R.; Martin, C. R.; Yoneyama, H. *J. Electrochem. Soc.* **1997**, *144*, 4296.
(30) Kang, M.; Trofin, L.; Mota, M. O.; Martin, C. R. *Anal. Chem.* **2005**, *77*, 6243.
(31) Kang, M.; Yu, S.; Li, N.; Martin, C. R. *Small* **2005**, *1*, 69.
(32) Chen, L.; Yin, A.; Im, J. S.; Nurmikko, A. V.; Xu, J. M.; Han, J. *Phys. Status Solidi A: Appl. Res.* **2001**, *188*, 135.
(33) Masuda, H.; Yasui, K.; Watanabe, M.; Nishio, K.; Rao, T. N.; Fujishima, A. *Chem. Lett.* **2000**, *29*, 1112.
(34) Che, G.; Lakshmi, B. B.; Martin, C. R.; Fisher, E. R.; Ruoff, R. S. *Chem. Mater.* **1998**, *10*, 260.
(35) Li, J.; Papadopoulos, C.; Xu, J. M.; Moskovits, M. *Appl. Phys. Lett.* **1999**, *75*, 367.
(36) Klein, J. D.; Herrick Ii, R. D.; Palmer, D.; Sailor, M. J.; Brumlik, C. J.; Martin, C. R. *Chem. Mater.* **1993**, *5*, 902.
(37) Lee, Y. H.; Leu, I. C.; Liao, C. L.; Chang, S. T.; Wu, M. T.; Yen, J. H.; Fung, K. Z. *Electrochem. Solid-State Lett.* **2006**, *9*, 207.
(38) Zhou, Y.; Shen, C.; Li, H. *Solid State Ionics* **2002**, *146*, 81.
(39) Li, N. C.; Patrissi, C. J.; Che, G. L.; Martin, C. R. *J. Electrochem. Soc.* **2000**, *147*, 2044.
(40) Xu, J. M. *Infrared Phys. Technol.* **2001**, *42*, 485.
(41) Polyakov, B.; Daly, B.; Prikulis, J.; Lisauskas, V.; Vengalis, B.; Morris, M. A.; Holmes, J. D.; Erts, D. *Adv. Mater.* **2006**, *18*, 1812.
(42) Nicewarner-Pena, S. R.; Freeman, R. G.; Reiss, B. D.; He, L.; Pena, D. J.; Walton, I. D.; Cromer, R.; Keating, C. D.; Natan, M. J. *Science* **2001**, *294*, 137.
(43) Hillebrenner, H.; Buyukserin, F.; Kang, M.; Mota, M. O.; Stewart, J. D.; Martin, C. R. *J. Am. Chem. Soc.* **2006**, *128*, 4236.
(44) Zoski, C. G.; Yang, N.; He, P.; Berdondini, L.; Koudelka-Hep, M. *Anal. Chem.* **2007**, *79*, 1474.
(45) Hulteen, J. C.; Martin, C. R. *J. Mater. Chem.* **1997**, *7*, 1075.
(46) Ugo, P.; Pepe, N.; Moretto, L. M.; Battagliarin, M. *J. Electroanal. Chem.* **2003**, *560*, 51.
(47) Gasparac, R.; Taft, B. J.; Lapierre-Devlin, M. A.; Lazareck, A. D.; Xu, J. M.; Kelley, S. O. *J. Am. Chem. Soc.* **2004**, *126*, 12270.
(48) Lapierre-Devlin, M. A.; Asher, C. L.; Taft, B. J.; Gasparac, R.; Roberts, M. A.; Kelley, S. O. *Nano Lett.* **2005**, *5*, 1051.
(49) Lapierre, M. A.; O'Keefe, M.; Taft, B. J.; Kelley, S. O. *Anal. Chem.* **2003**, *75*, 6327.
(50) Andreu, A.; Merkert, J. W.; Lecaros, L.; Broglin, B. L.; Brazell, J. T.; El-Kouedi, M. *Sens. Actuators, B* **2006**, *114*, 1116.
(51) Koehne, J.; Li, J.; Cassell, A. M.; Chen, H.; Ye, Q.; Ng, H. T.; Han, J.; Meyyappan, M. *J. Mater. Chem.* **2004**, *14*, 676.
(52) Koehne, J.; Chen, H.; Li, J.; Cassell, A. M.; Ye, Q.; Ng, H. T.; Han, J.; Meyyappan, M. *Nanotechnology* **2003**, *14*, 1239.
(53) Szunerits, S.; Tam, J. M.; Thouin, L.; Amatore, C.; Walt, D. R. *Anal. Chem.* **2003**, *75*, 4382.
(54) Lowe, R. D.; Mani, R. C.; Baldwin, R. P.; Sunkara, M. K. *Electrochem. Solid-State Lett.* **2006**, *9*, 43.
(55) Willets, K. A.; Van Duyne, R. P. *Ann. Rev. Phys. Chem.* **2007**, *58*, 267.
(56) Zhao, J.; Zhang, X.; Yonzon, C. R.; Haes, A. J.; Van Duyne, R. P. *Nanomedicine* **2006**, *1*, 219.
(57) Zhang, X.; Whitney, A. V.; Zhao, J.; Hicks, E. M.; Van Duyne, R. P. *J. Nanosci. Nanotechnol.* **2006**, *6*, 1920.
(58) Hankus, M. E.; Li, H.; Gibson, G. J.; Cullum, B. M. *Anal. Chem.* **2006**, *78*, 7535.
(59) Li, J.; Kamata, K.; Watanabe, S.; Iyoda, T. *Adv. Mater.* **2007**, *19*, 1267.
(60) Haynes, C. L.; Van Duyne, R. P. *J. Phys. Chem. B* **2001**, *105*, 5599.
(61) Yonzon, C. R.; Stuart, D. A.; Zhang, X.; McFarland, A. D.; Haynes, C. L.; Van Duyne, R. P. *Talanta* **2005**, *67*, 438.
(62) Vo-Dinh, T. *Trends Anal. Chem.* **1998**, *17*, 557.
(63) Yonzon, C. R.; Jeoung, E.; Zou, S.; Schatz, G. C.; Mrksich, M.; Van Duyne, R. P. *J. Am. Chem. Soc.* **2004**, *126*, 12669.
(64) Endo, T.; Kerman, K.; Nagatani, N.; Takamura, Y.; Tamiya, E. *Anal. Chem.* **2005**, *77*, 6976.

(65) Endo, T.; Kerman, K.; Nagatani, N.; Hiepa, H. M.; Kim, D. K.; Yonezawa, Y.; Nakano, K.; Tamiya, E. *Anal. Chem.* **2006**, *78*, 6465.
(66) Haes, A. J.; Chang, L.; Klein, W. L.; Van Duyne, R. P. *J. Am. Chem. Soc.* **2005**, *127*, 2264.
(67) Stuart, D. A.; Yuen, J. M.; Shah, N.; Lyandres, O.; Yonzon, C. R.; Glucksberg, M. R.; Walsh, J. T.; Van Duyne, R. P. *Anal. Chem.* **2006**, *78*, 7211.
(68) Driskell, J. D.; Kwarta, K. M.; Lipert, R. J.; Porter, M. D.; Neill, J. D.; Ridpath, J. F. *Anal. Chem.* **2005**, *77*, 6147.
(69) Zhang, X.; Young, M. A.; Lyandres, O.; Van Duyne, R. P. *J. Am. Chem. Soc.* **2005**, *127*, 4484.
(70) Zhang, X.; Zhao, J.; Whitney, A. V.; Elam, J. W.; Van Duyne, R. P. *J. Am. Chem. Soc.* **2006**, *128*, 10304.
(71) Yan, F.; Vo-Dinh, T. *Sens. Actuators, B* **2007**, *121*, 61.
(72) Holtz, J. H.; Asher, S. A. *Nature* **1997**, *389*, 829.
(73) Serpe, M. J.; Kim, J.; Lyon, L. A. *Adv. Mater.* **2004**, *16*, 184.
(74) Kim, J.; Singh, N.; Lyon, L. A. *Angew. Chem., Intl. Ed.* **2006**, *45*, 1446.
(75) Petersen, K. E. *Proc. IEEE* **1982**, *70*, 420.
(76) Salaita, K.; Wang, Y.; Mirkin, C. A. *Nat. Nanotechnol.* **2007**, *2*, 145.
(77) Ginger, D. S.; Zhang, H.; Mirkin, C. A. *Angew. Chem., Int. Ed.* **2004**, *43*, 30.
(78) Piner, R. D.; Zhu, J.; Xu, F.; Hong, S.; Mirkin, C. A. *Science* **1999**, *283*, 661.
(79) Liu, X.; Zhang, Y.; Goswami, D. K.; Okasinski, J. S.; Salaita, K.; Sun, P.; Bedzyk, M. J.; Mirkin, C. A. *Science* **2005**, *307*, 1763.
(80) Nam, J.-M.; Han, S. W.; Lee, K.-B.; Liu, X.; Ratner, M. A.; Mirkin, C. A. *Angew. Chem., Int. Ed.* **2004**, *43*, 1246.
(81) Jiang, H.; Stupp, S. I. *Langmuir* **2005**, *21*, 5242.
(82) Su, M.; Liu, X.; Li, S.-Y.; Dravid, V. P.; Mirkin, C. A. *J. Am. Chem. Soc.* **2002**, *124*, 1560.
(83) Hong, S.; Zhu, J.; Mirkin, C. A. *Science* **1999**, *286*, 523.
(84) Lee, K.-B.; Lim, J.-H.; Mirkin, C. A. *J. Am. Chem. Soc.* **2003**, *125*, 5588.
(85) Lee, K.-B.; Park, S.-J.; Mirkin, C. A.; Smith, J. C.; Mrksich, M. *Science* **2002**, *295*, 1702.
(86) Lee, K.-B.; Kim, E.-Y.; Mirkin, C. A.; Wolinsky, S. M. *Nano Lett.* **2004**, *4*, 1869.
(87) Zhang, H.; Li, Z.; Mirkin, C. A. *Adv. Mater.* **2002**, *14*, 1472.
(88) Park, S.-J.; Taton, T. A.; Mirkin, C. A. *Science* **2002**, *295*, 1503.
(89) Lenhert, S.; Sun, P.; Wang, Y.; Fuchs, H.; Mirkin, C. A. *Small* **2007**, *3*, 71.
(90) Salaita, K.; Wang, Y.; Fragala, J.; Vega, R. A.; Liu, C.; Mirkin, C. A. *Angew. Chem., Int. Ed.* **2006**, *45*, 7220.
(91) Fodor, S. P.; Read, J. L.; Pirrung, M. C.; Stryer, L.; Lu, A. T.; Solas, D. *Science* **1991**, *251*, 767.
(92) McGall, G. H.; Barone, A. D.; Diggelmann, M.; Fodor, S. P. A.; Gentalen, E.; Ngo, N. *J. Am. Chem. Soc.* **1997**, *119*, 5081.
(93) Fodor, S. P.; Rava, R. P.; Huang, X. C.; Pease, A. C.; Holmes, C. P.; Adams, C. L. *Nature* **1993**, *364*, 555.
(94) Matsuzaki, H.; Dong, S.; Loi, H.; Di, X.; Liu, G.; Hubbell, E.; Law, J.; Berntsen, T.; Chadha, M.; Hui, H.; Yang, G.; Kennedy, G. C.; Webster, T. A.; Cawley, S.; Walsh, P. S.; Jones, K. W.; Fodor, S. P. A.; Mei, R. *Nat. Meth.* **2004**, *1*, 109.
(95) Dufva, M. *Biomol. Eng.* **2005**, *22*, 173.
(96) Singh-Gasson, S.; Green, R. D.; Yue, Y.; Nelson, C.; Blattner, F.; Sussman, M. R.; Cerrina, F. *Nat. Biotechnol.* **1999**, *17*, 974.
(97) Nuwaysir, E. F.; Huang, W.; Albert, T. J.; Singh, J.; Nuwaysir, K.; Pitas, A.; Richmond, T.; Gorski, T.; Berg, J. P.; Ballin, J.; McCormick, M.; Norton, J.; Pollock, T.; Sumwalt, T.; Butcher, L.; Porter, D.; Molla, M.; Hall, C.; Blattner, F.; Sussman, M. R.; Wallace, R. L.; Cerrina, F.; Green, R. D. *Gen. Res.* **2002**, *12*, 1749.
(98) Naiser, T.; Mai, T.; Michel, W.; Ott, A. *Rev. Sci. Instrum.* **2006**, *77*, 063711/1.
(99) Lipshutz, R. J.; Fodor, S. P. A.; Gingeras, T. R.; Lockhart, D. J. *Nat. Gen.* **1999**, *21*, 20.
(100) Harrington, C. A.; Rosenow, C.; Retief, J. *Curr. Opin. Microbiol.* **2000**, *3*, 285.
(101) Lockhart, D. J.; Dong, H.; Byrne, M. C.; Follettie, M. T.; Gallo, M. V.; Chee, M. S.; Mittmann, M.; Wang, C.; Kobayashi, M.; Horton, H.; Brown, E. L. *Nat. Biotechnol.* **1996**, *14*, 1675.
(102) Wodicka, L.; Dong, H.; Mittmann, M.; Ho, M.-H.; Lockhart, D. J. *Nat. Biotechnol.* **1997**, *15*, 1359.
(103) Zaharik, M. L.; Nayar, T.; White, R.; Ma, C.; Vallance, B. A.; Straka, N.; Jiang, X.; Rey-Ladino, J.; Shen, C.; Brunham, R. C. *Immunology* **2007**, *120*, 160.
(104) Dame, T. M.; Orenzoff, B. L.; Palmer, L. E.; Furie, M. B. *J. Immunol.* **2007**, *178*, 1172.
(105) Takaishi, S.; Wang, T. C. *Cancer Sci.* **2007**, *98*, 284.
(106) Chang, W. L. W.; Coro, E. S.; Rau, F. C.; Xiao, Y.; Erle, D. J.; Baumgarth, N. *J. Immunol.* **2007**, *178*, 1457.
(107) Kruglyak, L.; Nickerson, D. A. *Nat. Gen.* **2001**, *27*, 234.
(108) Kennedy, G. C.; Matsuzaki, H.; Dong, S.; Liu, W.-m.; Huang, J.; Liu, G.; Su, X.; Cao, M.; Chen, W.; Zhang, J.; Liu, W.; Yang, G.; Di, X.; Ryder, T.; He, Z.; Surti, U.; Phillips, M. S.; Boyce-Jacino, M. T.; Fodor, S. P. A.; Jones, K. W. *Nat. Biotechnol.* **2003**, *21*, 1233.
(109) Yuan, E.; Haghighi, F.; White, S.; Costa, R.; McMinn, J.; Chun, K.; Minden, M.; Tycko, B. *Cancer Res.* **2006**, *66*, 3443.
(110) Britta Stordal, G. P. R. D. *Genes Chromosomes Cancer* **2006**, *45*, 1094.
(111) Cao, X.; Eu, K. W.; Kumarasinghe, M. P.; Li, H. H.; Loi, C.; Cheah, P. Y. *J. Med. Genet.* **2006**, *43*, e13.
(112) Calhoun, E. S.; Hucl, T.; Gallmeier, E.; West, K. M.; Arking, D. E.; Maitra, A.; Iacobuzio-Donahue, C. A.; Chakravarti, A.; Hruban, R. H.; Kern, S. E. *Cancer Res.* **2006**, *66*, 7920.
(113) Brown, P. O.; Botstein, D. *Nat. Gen.* **1999**, *21*, 33.
(114) Lockhart, D. J.; Winzeler, E. A. *Nature* **2000**, *405*, 827.
(115) Fan, J.-B.; Chee, M. S.; Gunderson, K. L. *Nat. Rev. Genet.* **2006**, *7*, 632.
(116) Bergveld, P. *Sens. Actuators, B* **2003**, *B88*, 1.
(117) Reinhoudt, D. N.; Engbersen, J. F. J.; Brzozka, Z.; van der Vlekkert, H. H.; Honig, G. W. N.; Holterman, H. A. J.; Verkerk, U. H. *Anal. Chem.* **1994**, *66*, 3618.
(118) Rochefeuille, S.; Jimenez, C.; Tingry, S.; Seta, P.; Desfours, J. P. *Mater. Sci. Eng. C: Biomimetic Supramol. Syst.* **2002**, *C21*, 43.
(119) Sant, W.; Pourciel, M. L.; Launay, J.; Do Conto, T.; Martinez, A.; Temple-Boyer, P. *Sens. Actuators, B* **2003**, *95*, 309.
(120) van der Schoot, B. H.; Bergveld, P. *Biosensors* **1988**, *3*, 161.
(121) Caras, S.; Janata, J. *Anal. Chem.* **1980**, *52*, 1935.
(122) Han, Y.; Offenhausser, A.; Ingebrandt, S. *Surf. Interface Anal.* **2006**, *38*, 176.
(123) Uslu, F.; Ingebrandt, S.; Mayer, D.; Bocker-Meffert, S.; Odenthal, M.; Offenhausser, A. *Biosens. Bioelectron.* **2004**, *19*, 1723.
(124) Yeow, T. C. W.; Haskard, M. R.; Mulcahy, D. E.; Seo, H. I.; Kwon, D. H. *Sens. Actuators, B* **1997**, *44*, 434.
(125) Allen, B. L.; Kichambare, P. D.; Star, A. *Adv. Mater.* **2007**, *19*, 1439.
(126) Deleted in proof.
(127) Patolsky, F.; Zheng, G.; Lieber, C. M. *Anal. Chem.* **2006**, *78*, 4260.
(128) Patolsky, F.; Timko, B. P.; Zheng, G.; Lieber, C. M. *MRS Bull.* **2007**, *32*, 142.
(129) Cui, Y.; Wei, Q.; Park, H.; Lieber, C. M. *Science* **2001**, *293*, 1289.
(130) Deleted in proof.
(131) Deleted in proof.
(132) Deleted in proof.
(133) Deleted in proof.
(134) Carlen, E. T.; van der Berg, A. *Lab Chip* **2006**, *7*, 19.
(135) Wang, W. U.; Chen, C.; Lin, K.-h.; Fang, Y.; Lieber, C. M. *PNAS* **2005**, *102*, 3208.
(136) Hahm, J.-i.; Lieber, C. M. *Nano Lett.* **2004**, *4*, 51.
(137) Deleted in proof.
(138) Li, Z.; Chen, Y.; Li, X.; Kamins, T. I.; Nauka, K.; Williams, R. S. *Nano Lett.* **2004**, *4*, 245.
(139) Li, Z.; Rajendran, B.; Kamins, T. I.; Li, X.; Chen, Y.; Williams, R. S. *Appl. Phys. A: Mater. Sci. Process.* **2005**, *80*, 1257.
(140) Stern, E.; Klemic, J. F.; Routenberg, D. A.; Wyrembak, P. N.; Turner-Evans, D. B.; Hamilton, A. D.; LaVan, D. A.; Fahmy, T. M.; Reed, M. A. *Nature* **2007**, *445*, 519.
(141) Bunimovich, Y. L.; Shin, Y. S.; Yeo, W.-S.; Amori, M.; Kwong, G.; Heath, J. R. *J. Am. Chem. Soc.* **2006**, *128*, 16323.
(142) Wang, D.; Sheriff, B. A.; Heath, J. R. *Nano Lett.* **2006**, *6*, 1096.
(143) Patolsky, F.; Zheng, G.; Hayden, O.; Lakadamyali, M.; Zhuang, X.; Lieber, C. M. *PNAS* **2004**, *101*, 14017.
(144) Zheng, G.; Patolsky, F.; Cui, Y.; Wang, W. U.; Lieber, C. M. *Nat. Biotechnol.* **2005**, *23*, 1294.
(145) Deleted in proof.
(146) Steemers, F. J.; Walt, D. R. *Mikrochim. Acta* **1999**, *131*, 99.
(147) Walt, D. R. *Curr. Opin. Chem. Biol.* **2002**, *6*, 689.
(148) Epstein, J. R.; Walt, D. R. *Chem. Soc. Rev.* **2003**, *32*, 203.
(149) Walt, D. R. *Science* **2000**, *287*, 451.
(150) Epstein, J. R.; Leung, A. P. K.; Lee, K.-H.; Walt, D. R. *Biosens. Bioelectron.* **2003**, *18*, 541.
(151) Ferguson, J. A.; Steemers, F. J.; Walt, D. R. *Anal. Chem.* **2000**, *72*, 5618.
(152) Dickinson, T. A.; Michael, K. L.; Kauer, J. S.; Walt, D. R. *Anal. Chem.* **1999**, *71*, 2192.
(153) Gunderson, K. L.; Kruglyak, S.; Graige, M. S.; Garcia, F.; Kermani, B. G.; Zhao, C.; Che, D.; Dickinson, T.; Wickham, E.; Bierle, J.; Doucet, D.; Milewski, M.; Yang, R.; Siegmund, C.; Haas, J.; Zhou, L.; Oliphant, A.; Fan, J.-B.; Barnard, S.; Chee, M. S. *Gen. Res.* **2004**, *14*, 870.
(154) Song, L.; Ahn, S.; Walt, D. R. *Anal. Chem.* **2006**, *78*, 1023.
(155) Epstein, J. R.; Lee, M.; Walt, D. R. *Anal. Chem.* **2002**, *74*, 1836.
(156) Bowden, M.; Song, L.; Walt, D. R. *Anal. Chem.* **2005**, *77*, 5583.
(157) Shepard, J. R. E.; Danin-Poleg, Y.; Kashi, Y.; Walt, D. R. *Anal. Chem.* **2005**, *77*, 319.

(158) Steemers, F. J.; Ferguson, J. A.; Walt, D. R. *Nat. Biotechnol.* **2000**, *18*, 91.
(159) Ahn, S.; Walt, D. R. *Anal. Chem.* **2005**, *77*, 5041.
(160) Ahn, S.; Kulis, D. M.; Erdner, D. L.; Anderson, D. M.; Walt, D. R. *Appl. Environ. Microbiol.* **2006**, *72*, 5742.
(161) Epstein, J. R.; Ferguson, J. A.; Lee, K.-H.; Walt, D. R. *J. Am. Chem. Soc.* **2003**, *125*, 13753.
(162) Kuhn, K.; Baker, S. C.; Chudin, E.; Lieu, M.-H.; Oeser, S.; Bennett, H.; Rigault, P.; Barker, D.; McDaniel, T. K.; Chee, M. S. *Gen. Res.* **2004**, *14*, 2347.
(163) Fan, J.-B.; Yeakley, J. M.; Bibikova, M.; Chudin, E.; Wickham, E.; Chen, J.; Doucet, D.; Rigault, P.; Zhang, B.; Shen, R.; McBride, C.; Li, H.-R.; Fu, X.-D.; Oliphant, A.; Barker, D. L.; Chee, M. S. *Gen. Res.* **2004**, *14*, 878.
(164) Gelder, R. N. V.; von Zastrow, M. E.; Yool, A.; Dement, W. C.; Barchas, J. D.; Eberwine, J. H. *PNAS* **1990**, *87*, 1663.
(165) Shen, R.; Fan, J.-B.; Campbell, D.; Chang, W.; Chen, J.; Doucet, D.; Yeakley, J.; Bibikova, M.; Wickham Garcia, E.; McBride, C.; Steemers, F.; Garcia, F.; Kermani, B. G.; Gunderson, K.; Oliphant, A. *Mut. Res. Fund. Mole. Mech. of Mutagen.* **2005**, *573*, 70.
(166) Steemers, F. J.; Gunderson, K. L. *Biotechnol. J.* **2007**, *2*, 41.
(167) Lee, M.; Walt, D. R. *Anal. Biochem.* **2000**, *282*, 142.
(168) Adams, E. W.; Ueberfeld, J.; Ratner, D. M.; O'Keefe, B. R.; Walt, D. R.; Seeberger, P. H. *Angew. Chem., Int. Ed.* **2003**, *42*, 5317.
(169) Szurdoki, F.; Michael, K. L.; Walt, D. R. *Anal. Biochem.* **2001**, *291*, 219.
(170) Rissin, D. M.; Walt, D. R. *Anal. Chim. Acta* **2006**, *564*, 34.
(171) Rissin, D. M.; Walt, D. R. *Nano Lett.* **2006**, *6*, 520.
(172) Rissin, D. M.; Walt, D. R. *J. Am. Chem. Soc.* **2006**, *128*, 6286.
(173) Bigos, M.; Baumgarth, N.; Jager, G. C.; Herman, O. C.; Nozaki, T.; Stovel, R. T.; Parks, D. R.; Herzenberg, L. A. *Cytometry* **1999**, *36*, 36.
(174) Deutsch, A.; Zurgil, N.; Hurevich, I.; Shafran, Y.; Afrimzon, E.; Lebovich, P.; Deutsch, M. *Biomed. Microdev.* **2006**, *8*, 361.
(175) Taylor, L. C.; Walt, D. R. *Anal. Biochem.* **2000**, *278*, 132.
(176) Fink, J.; Thery, M.; Azioune, A.; Dupont, R.; Chatelain, F.; Bornens, M.; Piel, M. *Lab Chip* **2007**, *7*, 672.
(177) Khademhosseini, A.; Langer, R.; Borenstein, J.; Vacanti, J. P. *PNAS* **2006**, *103*, 2480.
(178) Chen, C. S.; Mrksich, M.; Huang, S.; Whitesides, G. M.; Ingber, D. E. *Science* **1997**, *276*, 1425.
(179) Ostuni, E.; Chen, C. S.; Ingber, D. E.; Whitesides, G. M. *Langmuir* **2001**, *17*, 2828.
(180) Kandere-Grzybowska, K.; Campbell, C. J.; Mahmud, G.; Komarova, Y.; Soh, S.; Grzybowski, B. A. *Soft Matter* **2007**, *3*, 672.
(181) Greve, F.; Lichtenberg, J.; Hierlemann, A. *IEEE Sens.* **2004**, 80.
(182) Kuang, Y.; Biran, I.; Walt, D. R. *Anal. Chem.* **2004**, *76*, 2902.
(183) Biran, I.; Walt, D. R. *Anal. Chem.* **2002**, *74*, 3046.
(184) Kuang, Y.; Biran, I.; Walt, D. R. *Anal. Chem.* **2004**, *76*, 6282.
(185) Dragoy Whitaker, R.; Walt, D. R. *Anal. Biochem.* **2007**, *360*, 63.
(186) Biran, I.; Rissin, D. M.; Ron, E. Z.; Walt, D. R. *Anal. Biochem.* **2003**, *315*, 106.
(187) DiCesare, C.; Biran, I.; Walt, D. R. *Anal. Bioanal. Chem.* **2005**, *382*, 37.
(188) Yamamura, S.; Kishi, H.; Tokimitsu, Y.; Kondo, S.; Honda, R.; Rao, S. R.; Omori, M.; Tamiya, E.; Muraguchi, A. *Anal. Chem.* **2005**, *77*, 8050.
(189) www.molecular-cytomics.com.
(190) Albert, K. J.; Lewis, N. S.; Schauer, C. L.; Sotzing, G. A.; Stitzel, S. E.; Vaid, T. P.; Walt, D. R. *Chem. Rev.* **2000**, *100*, 2595.
(191) Dickinson, T. A.; White, J.; Kauer, J. S.; Walt, D. R. *Trends Biotechnol.* **1998**, *16*, 250.
(192) Stitzel, S. E.; Stein, D. R.; Walt, D. R. *J. Am. Chem. Soc.* **2003**, *125*, 3684.
(193) Albert, K. J.; Myrick, M. L.; Brown, S. B.; James, D. L.; Milanovich, F. P.; Walt, D. R. *Environ. Sci. Technol.* **2001**, *35*, 3193.
(194) Lundstrom, I.; Shivaraman, S.; Svensson, C.; Lundkvist, L. *Appl. Phys. Lett.* **1975**, *26*, 55.
(195) Persaud, K.; Dodd, G. *Nature* **1982**, *299*, 352.
(196) McAlpine, M. C.; Ahmad, H.; Wang, D.; Heath, J. R. *Nat. Mater.* **2007**, *6*, 379.
(197) Pearce, T. C.; Gardner, J. W.; Friel, S.; Bartlett, P. N.; Blair, N. *Analyst* **1993**, *118*, 371.
(198) Legin, A. V.; Vlasov, Y. G.; Rudnitskaya, A. M.; Bychkov, E. A. *Sens. Actuators, B* **1996**, *B34*, 456.
(199) Amati, D.; Arn, D.; Blom, N.; Ehrat, M.; Saunois, J.; Widmer, H. M. *Sens. Actuators, B* **1992**, *B7*, 587.
(200) Burns, J. A.; Whitesides, G. M. *Chem. Rev.* **1993**, *93*, 2583.
(201) Albert, K. J.; Walt, D. R. *Anal. Chem.* **2003**, *75*, 4161.
(202) Stitzel, S. E.; Cowen, L. J.; Albert, K. J.; Walt, D. R. *Anal. Chem.* **2001**, *73*, 5266.
(203) Bencic-Nagale, S.; Walt, D. R. *Anal. Chem.* **2005**, *77*, 6155.
(204) Albert, K. J.; Walt, D. R. *Anal. Chem.* **2000**, *72*, 1947.
(205) Albert, K. J.; Walt, D. R.; Gill, D. S.; Pearce, T. C. *Anal. Chem.* **2001**, *73*, 2501.
(206) Horan, P. K.; Wheeless, L. L., Jr. *Science* **1977**, *198*, 149.
(207) Vignali, D. A. A. *J. Immunol. Methods* **2000**, *243*, 243.
(208) Nolan, J. P.; Sklar, L. A. *Nat. Biotechnol.* **1998**, *16*, 633.
(209) Nolan, J. P.; Sklar, L. A. *Trends Biotechnol.* **2002**, *20*, 9.
(210) Wilson, R.; Cossins, A. R.; Spiller, D. G. *Angew. Chem., Int. Ed.* **2006**, *45*, 6104.
(211) Finkel, N. H.; Lou, X.; Wang, C.; He, L. *Anal. Chem.* **2004**, *76*, 352A.
(212) He, B.; Son, S. J.; Lee, S. B. *Anal. Chem.* **2007**, *79*, 5257.
(213) He, B.; Son, S. J.; Lee, S. B. *Langmuir* **2006**, *22*, 8263.
(214) Pregibon, D. C.; Toner, M.; Doyle, P. S. *Science* **2007**, *315*, 1393.
(215) www.luminexcorp.com.
(216) McHugh, T. M.; Stites, D. P.; Casavant, C. H.; Fulwyler, M. J. *J. Immunol. Methods* **1986**, *95*, 57.
(217) McHugh, T. M.; Miner, R. C.; Logan, L. H.; Stites, D. P. *J. Clin. Microbiol.* **1988**, *26*, 1957.
(218) Saunders, G. C.; Jett, J. H.; Martin, J. C. *Clin. Chem.* **1985**, *31*, 2020.
(219) Fulton, R. J.; McDade, R. L.; Smith, P. L.; Kienker, L. J.; Kettman, J. R., Jr. *Clin. Chem.* **1997**, *43*, 1749.
(220) Carson, R. T.; Vignali, D. A. A. *J. Immunol. Methods* **1999**, *227*, 41.
(221) Dasso, J.; Lee, J.; Bach, H.; Mage, R. G. *J. Immunol. Methods* **2002**, *263*, 23.
(222) Yamamoto, K.; Ito, S.; Yasukawa, F.; Konami, Y.; Matsumoto, N. *Anal. Biochem.* **2005**, *336*, 28.
(223) Goldman, E. R.; Anderson, G. P.; Liu, J. L.; Delehanty, J. B.; Sherwood, L. J.; Osborn, L. E.; Cummins, L. B.; Hayhurst, A. *Anal. Chem.* **2006**, *78*, 8245.
(224) Anderson, G. P.; Moreira, S. C.; Charles, P. T.; Medintz, I. L.; Goldman, E. R.; Zeinali, M.; Taitt, C. R. *Anal. Chem.* **2006**, *78*, 2279.
(225) Martinelli, E.; Cicala, C.; Van Ryk, D.; Goode, D. J.; Macleod, K.; Arthos, J.; Fauci, A. S. *PNAS* **2007**, *104*, 3396.
(226) Kobasa, D.; Jones, S. M.; Shinya, K.; Kash, J. C.; Copps, J.; Ebihara, H.; Hatta, Y.; Kim, J. H.; Halfmann, P.; Hatta, M.; Feldmann, F.; Alimonti, J. B.; Fernando, L.; Li, Y.; Katze, M. G.; Feldmann, H.; Kawaoka, Y. *Nature* **2007**, *445*, 319.
(227) Yang, L.; Tran, D. K.; Wang, X. *Genome Res.* **2001**, *11*, 1888.
(228) Lu, J.; Getz, G.; Miska, E. A.; Alvarez-Saavedra, E.; Lamb, J.; Peck, D.; Sweet-Cordero, A.; Ebert, B. L.; Mak, R. H.; Ferrando, A. A.; Downing, J. R.; Jacks, T.; Horvitz, H. R.; Golub, T. R. *Nature* **2005**, *435*, 834.
(229) Flagella, M.; Bui, S.; Zheng, Z.; Nguyen, C. T.; Zhang, A.; Pastor, L.; Ma, Y.; Yang, W.; Crawford, K. L.; McMaster, G. K.; Witney, F.; Luo, Y. *Anal. Biochem.* **2006**, *352*, 50.
(230) Armstrong, B.; Stewart, M.; Mazumder, A. *Cytometry* **2000**, *40*, 102.
(231) Iannone, M. A.; Taylor, J. D.; Chen, J.; Li, M.-S.; Rivers, P.; Slentz-Kesler, K. A.; Weiner, M. P. *Cytometry* **2000**, *39*, 131.
(232) Chen, J.; Iannone, M. A.; Li, M.-S.; Taylor, J. D.; Rivers, P.; Nelsen, A. J.; Slentz-Kesler, K. A.; Roses, A.; Weiner, M. P. *Genome Res.* **2000**, *10*, 549.
(233) Cai, H.; White, P. S.; Torney, D.; Deshpande, A.; Wang, Z.; Marrone, B.; Nolan, J. P. *Genomics* **2000**, *66*, 135.
(234) Bayley, H.; Martin, C. R. *Chem. Rev.* **2000**, *100*, 2575.
(235) Wharton, J. E.; Jin, P.; Sexton, L. T.; Horne, L. P.; Sherrill, S. A.; Mino, W. K.; Martin, C. R. *Small* **2007**, *3*, 1424.
(236) Shao, M.-W.; Shan, Y.-Y.; Wong, N.-B.; Lee, S.-T. *Adv. Funct. Mater.* **2005**, *15*, 1478.
(237) Star, A.; Tu, E.; Niemann, J.; Gabriel, J.-C. P.; Joiner, C. S.; Valcke, C. *PNAS* **2006**, *103*, 921.
(238) Sirbuly, D. J.; Tao, A.; Law, M.; Fan, R.; Yang, P. *Adv. Mater.* **2007**, *19*, 61.
(239) Zhao, X.; Cao, Y.; Ito, F.; Chen, H.-H.; Nagai, K.; Zhao, Y.-H.; Gu, Z.-Z. *Angew. Chem., Int. Ed.* **2006**, *45*, 6835.
(240) Kuncicky, D. M.; Prevo, B. G.; Velev, O. D. *J. Mater. Chem.* **2006**, *16*, 1207.
(241) Claridge, S. A.; Goh, S. L.; Frechet, J. M. J.; Williams, S. C.; Micheel, C. M.; Alivisatos, A. P. *Chem. Mater.* **2005**, *17*, 1628.
(242) Cha, J. N.; Zhang, Y.; Wong, H. S. P.; Raoux, S.; Rettner, C.; Krupp, L.; Deline, V. *Chem. Mater.* **2007**, *19*, 839.
(243) McFarland, A. D.; Van Duyne, R. P. *Nano Lett.* **2003**, *3*, 1057.
(244) Wang, Z. L.; Song, J. *Science* **2006**.
(245) Angelos, S.; Johansso, E.; Stoddart, J. F.; Zink, J. I. *Adv. Funct. Mater.* **2007**, *17*, 2261.
(246) Nguyen, T. D.; Liu, Y.; Saha, S.; Leung, K. C.; Stoddart, J. F.; Zink, J. I. *J. Am. Chem. Soc.* **2007**, *129*, 626.
(247) Stoddart, J. F.; Zink, J. I. *Adv. Funct. Mater.* **2007**, *17*, 685.
(248) Sidorenko, A.; Krupenkin, T.; Taylor, A.; Fratzl, P.; Aizenberg, J. *Science* **2007**, *315*, 487.
(249) Gu, L. Q.; Cheley, S.; Bayley, H. *Science* **2001**, *291*, 636.
(250) Seeman, N. C. *Chem. Biol.* **2003**, *10*, 1151.
(251) Seeman, N. C. *Nature* **2003**, *421*, 427.

(252) Grier, D. G.; Roichman, Y. *Appl. Opt.* **2006**, *45*, 880.
(253) Tam, J. M.; Biran, I.; Walt, D. R. *Appl. Phys. Lett.* **2004**, *84*, 4289.
(254) Willig, K. I.; Rizzoli, S. O.; Westphal, V.; Jahn, R.; Hell, S. W. *Nature* **2006**, *440*, 935.
(255) Klar, T. A.; Jakobs, S.; Dyba, M.; Egner, A.; Hell, S. W. *PNAS* **2000**, *97*, 8206.
(256) Rust, M. J.; Bates, M.; Zhuang, X. *Nat. Meth.* **2006**, *3*, 793.
(257) Bates, M.; Huang, B.; Dempsey, G. T.; Zhuang, X. *Science* **2007**, *317*, 1749.
(258) Smith, C. *Nature* **2007**, *446*, 219.
(259) Staples, M.; Daniel, K.; Cima, M. J.; Langer, R. *Pharmacol. Res.* **2006**, *23*, 847.
(260) Sigworth, F. J.; Klemic, K. G. *Biophys. J.* **2002**.
(261) Buxboim, A.; Bar-Dagan, M.; Frydman, V.; Zbaida, D.; Morpurgo, M.; Bar-Ziv, R. *Small* **2007**, *3*, 500.
(262) Maerkl, S. J.; Quake, S. R. *Science* **2007**, *315*, 233.
(263) Margulies, M.; Egholm, M.; Altman, W. E.; Attiya, S.; Bader, J. S.; Bemben, L. A.; Berka, J.; Braverman, M. S.; Chen, Y. J.; Chen, Z. *Nature* **2005**, *437*, 376.
(264) Bentley, D. R. *Curr. Opin. Genet. Dev.* **2006**, *16*, 545.
(265) Malek, J. A.; Wierzbowski, J. M.; Tao, W.; Bosak, S. A.; Saranga, D. J.; Doucette-Stamm, L.; Smith, D. R.; McEwan, P. J.; McKernan, K. J. *Nucleic Acids Res.* **2004**, *32*, 1059.
(266) Harris, T.; Buzby, P. R.; Jarosz, M.; Dimeo, J. J.; Gill, J. (Helicos Biosciences Corp., U.S.A.). WO Patent Application, 2006.
(267) Teo, B. K.; Sun, X. H. *Chem. Rev.* **2007**, *107*, 1454.
(268) Collins, S.; Janata, J. *Anal. Chim. Acta* **1982**, *136*, 93.
(269) Janata, J.; Blackburn, G. F. *Ann. N. Y. Acad. Sci.* **1984**, *428*, 286.
(270) Janata, J. *Principles of Chemical Sensors*; Plenum Press: New York, 1989.
(271) Bradley, K.; Gabriel, J.-C. P.; Star, A.; Gruener, G. *Appl. Phys. Lett.* **2003**, *83*, 3821.
(272) Minot, E. D.; Janssens, A. M.; Heller, I.; Heering, H. A.; Dekker, C.; Lemay, S. G. *Appl. Phys. Lett.* **2007**, *91*, 093507/1.
(273) Stern, E.; Wagner, R.; Sigworth, F. J.; Breaker, R.; Fahmy, T. M.; Reed, M. A. *Nano Lett.* **2007**, *7*, 3405.

CR0681142